



**3D&FPP**



## Integrating Metal 3D Printing & Flexible Post Processing

### O 2.1 – Feasibility test

<b>Partners</b>	TNO, HR, Hittech, 3T, Exeter and Argon
<b>Authors</b>	TNO, Peter Giesen TNO, Richard van Lieshout TNO, Edwin van den Eijnden Hittech Multin, Jeroen Valentijn Hittech Multin, Richard Pieper University of Exeter, Qiang Li Argon Measuring Services, Frederik Oprins
<b>Contributors (Authors)</b>	All partners
<b>Checked by</b>	Hogeschool Rotterdam, Mariëlle van Dijk
<b>Date of delivery</b>	31.01.2018
<b>Document version</b>	V1.1

Application form: **2S01097 3D&FPP**

Programme priority specific objective: **SO 1.2 Increase the delivery of innovation in smart specialisation sectors**

Program priority: **1. Technological and social innovation**

Start date of the project: **01.09.2016**

Duration: **40 months**

## CHANGE CONTROL

Revision	Status	Date	Comment
V0.1	Draft	20171219	First draft of merged document
V0.2	Draft	20171219	Update
V0.3	Draft	20171219	Update
V0.4	Draft	20180122	Update
V0.5	Draft	20180124	Update Edwin van den Eijnden
V0.6	Draft	20180125	Update Edwin van den Eijnden
V0.7	Draft	20180125	Update Edwin van den Eijnden
v0.8	Draft	20180129	Update Edwin van den Eijnden
V1.0	Final	20180131	

## APPLICABLE & REFERENCE DOCUMENTS

Ref.	Document title	Author	Doc Id	Status	Date
RD01	Application Form	Interreg	3D&FPP_ApplicationForm_final.pdf	Submitted	20170720
RD02	O 1.1 Feasibility study/preparatory research report	TNO, HR, Hittech, 3T, Exeter and Argon			

## APPLICATION FORM

Activity/ deliverable	Title	Description	Delivery month
O 2.1	Feasibility test	The feasibility test will be performed on a simple shape of a 3D printed metal component. The test result will measure the accuracy of the key components of the post processing tool and process that will be developed in WP2. The result of the test will progress the envisaged development from TRL level 3 to 5.	20171231

# TABLE OF CONTENTS

1	Executive summary .....	5
2	Introduction .....	7
2.1	Fast prototyping approach [RD02] .....	8
2.1.1	Introduction.....	8
2.1.2	Approach .....	8
3	Feasibility test .....	10
3.1	Clamping.....	10
3.1.1	Concept 1: printing extra handles .....	10
3.1.2	Concept 2: clamping with hotmelt .....	14
3.1.3	Concept 3: softclamp based on bed of pins .....	23
3.1.4	Concept 4: printing on an extra base plate .....	26
3.2	Scanning .....	28
3.2.1	Accuracy & Repeatability .....	28
3.2.2	Automation potential.....	29
3.2.3	Processing 3D data for milling machine compensation .....	30
3.2.4	Future tests .....	33
3.3	Polishing .....	33
3.3.1	Test domeless rotary vibrator .....	33
3.3.2	Future tests .....	38
3.4	CAD -CAM .....	39
3.4.1	Definition of the feasibility test.....	39
3.4.2	Calculation of required parameters .....	41
3.4.3	Validation of the proposed method .....	43
4	Conclusion .....	45
5	Annexes .....	47
5.1	List of figures .....	47
5.2	List of tables .....	48
6	Appendix A: Polishing challenges marked in drawing .....	49
6.1	Appendix A.1: Drawing Cooling Core .....	49
6.2	Appendix A.2: Drawing Gearbox Design.....	50
6.3	Appendix A.3: Drawing Fokker Hinge .....	51



# 1 EXECUTIVE SUMMARY

3D metal printing is an emerging technology that allows new designs. It enables for example the development of lighter products or with higher cooling performance. The products quality as build is comparable with casted products. These products have to be post processed in order to realize accuracy or surface roughness constrains.

Post processing costs add significantly to the total cost. Therefore focusing on only reducing the printing cost will not lead to an overall minimum cost.

The Interreg2seas 3D&FPP project focuses on the reduction of the post processing cost (30 %) and time (50 %) on the reduction of the post processing steps. The post processing steps that are taken into account are (re)clamping, scanning, CNC milling/drilling, polishing, unclamping and quality check.

In order to quantify the requirements, cost and time reduction, use cases were obtained from industrial observer partners. Based on these requirements, concepts were generated for clamping, scanning, polishing and CAD CAM. These concepts were described in the Output 1.1 document: Feasibility study preparatory reserach report. For some process steps still different options are open. In order to make a selection of the preferred and feasible concept, feasibility experiments were performed. The experiments and results are described in this document. Also in the remaining of the project further experiments will be performed to determine the performance of the post processing system. This output will describe the initial experiments to come to an initial selection.

## Fast prototyping approach

In the original proposal integrated tests with different process steps were mainly foreseen in WP3. However some integrated tests were already performed to show feasibility on an integrated level. The goal is also to speed-up the project.

## Clamping

The clamping concepts that were further investigated using experiments are:

- A special interface that is printed on the product, that can remain on the product or can be removed later.  
Experiments showed that it is possible to print clamping interfaces to printed objects. This gives more freedom in how to clamp the object. Objects that are printed free of defects are not guaranteed not to have defects with the additional clamping interface. Design rules should be developed for this. It is also important that the wall too which the interface is printed has enough stiffness.
- Hot melts  
Hot melt are found that are most likely strong enough to hold the object in place while milling. The initial experiments also show that the hot melts can be removed from the product leaving hardly any traces. The young's modulus of the material is however quite low and does not allow applying a thick layer.
- Softclamp based on bed of fins  
A Matrix clamp was obtained to perform more tests. Initial experiments of the technology seem promising. Other customers for the system are for example in the field of clamping castings. A part of the product is covered with the clamping tool and cannot be milled.

The preferred solution to proceed with is the special interface printed on the product and/or in combination with the soft clamp based on a bed of fins.

### Scanning

In order to post process a part the position and orientation of a part has to be known in relation to the milling coordinates. The product can be repositioned in the clamp, till it is in the right position in the milling system. Another approach would be to measure the position and orientation in the clamp and use this as input for the milling CAD/CAM software without repositioning the object.

Scanning tests were performed on a 3D printed object clamped in a certain position. With the scanner and software the position and orientation of the product were determined. Based on the measurements the hardware and software were qualified as suitable for the project scope. A second experiment was performed where the coordinates were used as compensation for the different coordinates of the milling system with the goal to mill a perfectly flat part. The surface was however not completely flat. Why is that will be further worked out next work packages.

### Polishing

Based on the polishing concepts, expected issues were determined and methods how to determine the performance. The polishing tests mainly focused on a domeless rotary vibrator that is a quite common technology in this field. As a next step test samples were designed and produced to measure the performance of the selected polishing techniques. Initial tests with the domeless rotary vibrator showed that the surface roughness of the products were out of specification. In cooperation with the manufacturer more experiments will be planned. For laser polishing and robotic supported polishing no supplier was found that could do the experiment.

### CAD/CAM

The university of Exeter and Hittech supported the second experiment as described in the scanning experiment paragraph. This experiment is not a standalone experiment anymore, evaluating one process step. It already gives indications of the integrated approach. The approach is called fast prototyping approach in this document. Based on the experiment there were lessons learned that will be used in future experiments to improve the method and the correction.

For the selection of the preferred post processing steps the TRL (Technology Readiness Level) level is an important criterion. Only technologies were selected that have a TRL level of at least 5.

## 2 INTRODUCTION

This report concludes the initial work package of the 3D&FPP project with feasibility test results. Focus during this initial phase has been identifying the 3D printing and post-processing production chain, as well as investigating the various techniques involved in the separate process steps.

It has been shown that in the opinion of the partners, the integrated post-process flow contains the following steps:

- Clamping the 3D printed product in a flexible manner;
- Scanning the printed product while it is clamped;
- Comparing the scanned data of the actual printed product with the desired end result of the customer, and;
- Converting the scanned data to be used in the subsequent milling and polishing steps.

Research on clamping has indicated several interesting technologies. These technologies have been scored on several aspects, and showing the following technologies are most promising:

- Printing of additional features which can be clamped;
- The use of Hot melt;
- The use of a bed of pens.

Some of these solutions are more suitable for a series product, while some excel for prototype products. The feasibility experiments for clamping are described in paragraph 3.1.

Scanning of the product was initially regarded to serve 2 purposes: 1) inspect the orientation of the printed product with respect to the clamp, and 2) perform the final quality check. It has been found however that performing a quality check with the required resolution and accuracy is not feasible with current state of the art scanning systems. Therefore the focus has been on using scanning technology to define the orientation of the product with respect to the clamp, such that this info can be used in a later stage of the process to for instance re-orientate the CNC machine bed. Feasibility experiments are performed to determine position and orientation. These tests are described in paragraph 3.2.

Investigation has shown that the following technologies look most promising for this purpose:

- Prototype / one-off: The use of a 3D Structured light system;
- Batch process: For the batch process a conclusive system could not be identified.

Three polishing techniques have been identified which are suitable to be integrated in the new manufacturing flow. These are:

- Domeless vibratory polishing;
- Robotic supported polishing;
- Laser polishing.

The techniques differ in their suitability to be used either for prototypes / one-off products on the one hand, and a series product on the other hand. The techniques are subject to testing in the subsequent project phase. A clever way of integrating all the separate process steps results in a reduction of production time and costs.

Integrating the position and orientation correction showed 2 integration concepts:

- Integration with CAM;
- Integration with CNC.

Initial integrated tests (fast prototyping approach) showed already more information to determine the optimal approach. This test is described in chapter 2 and paragraph 3.2.

Above mentioned concept solutions have been found with various concept generation techniques, literature studies and retrieving information from discussions with observers / market parties. The concepts have been scored with the aim to reduce production time with 50% production cost with 30% with respect to current manufacturing time and cost. Also the TRL level of the concept is an important selection criterion. Only concepts were selected that have a TRL level of at least 5.

Testing of the various concepts, and validating the reduction of time and costs will be realized in the remaining part of the project.

## **2.1 FAST PROTOTYPING APPROACH [RD02]**

### **2.1.1 INTRODUCTION**

In reference to the conclusions in Output document O 1.1 and the above Introduction, Hittech in cooperation with Argon en the University of Exeter, has conducted a test by using scanning, CAD and CNC data in an overall prototyping approach.

The goal of this approach was to verify whether machine settings could be updated with scanning and CAD data providing a new and accurate CNC positioning table.

Results of these tests can be found in the paragraph on Scanning.

### **2.1.2 APPROACH**

A clamp containing an object with a plain (Figure 1, left) of known reference with respect to the CNC zero point coordinate system was used. This clamp containing the object with the plain of known reference was scanned by Argon (Figure 1, right).

With this scanning data the offset values for the CNC machinery was calculated. Subsequently the calculated off set values for the CNC machinery was cross-referenced with the gauged off set values.

More detail on the tests results is shown in the paragraph on Scanning.



*Figure 1 left; the Fast Prototype object during fabrication by using a 5 axis CNC milling machine at Hitech Bihca. Right: The object during 3D scanning by using a robotized measuring cell at Argon measuring solutions*

## 3 FEASIBILITY TEST

### 3.1 CLAMPING

In the document O1.1 an overview is given of clamping concepts. Based on the trade-off table (see Table 1) the most promising concepts have been selected for feasibility tests.

Table 1: trade off table with clamping concepts.

	clamping stability	Clamp force	clamp time	declamp time	1st clamping	2nd clamping	clamping interface	tool accessibility	Environment	cost 30%	time 50%	remarks	total
baseplate modifications	5	5	5	1	5	1	3	3	5	3	3	1st clamping only	3.5
Printing extra interface													
Handle	3	3	5	4	5	4	3	4	5	3	3		3.8
Frame	3	3	5	4	5	3	3	3	5	3	3		3.6
struts	3	3	5	4	5	4	3	3	5	3	3		3.7
Liquid-solid													
liquid metal	4	4	4	4	5	5	4	4	2	4	4	commercial available	4.0
hot melt	?	?	5	4	5	5	3	4	2	5	5	fiber reinforced?	4.2
ice	3	3	5	5	5	5	2	3	2	3	3		3.5
cast	3	2	4	2	5	5	4	4	3	5	5		3.8
UV resin	4	4	5	1	4	4	4	4	5	3	4		3.8
softclamp													
clay afdruk	3	2	4	1	4	4	3	4	4	5	5		3.5
fill a thin gap	5	4	3	3	4	4	4	4	4	2	2		3.5
Bed of pins	4	4	5	5	4	4	5	3	5	4	4	commercial available/matrix	4.3
FDM print	4	4	2	3	5	5	3	4	3	2	2	fiber reinforced?	3.4
Press in a thermoplast	3	3	4	4	5	5	3	3	4	4	4		3.8
Other													
welding dots	4	4	4	3	5	3	4	3	4	4	4		3.8
UV curable glue dots	4	4	4	3	5	4	4	3	5	4	4		4.0

Based on the trade-off, four techniques were selected: printing extra handles, clamping with hotmelt, softclamp based on bed of pins and press in a thermoplast.

The hotmelt concept and the softclamp made by thermoplast are combined since the methods have in common that it comprises of low Young's modulus materials and both have the discussion of adhesion

An extra feasibility will be discussed with respect to Baseplate modifications. One of the options to print on a clamp plate that is mounted on the baseplate is excused via another project. The results will be shown.

#### 3.1.1 CONCEPT 1: PRINTING EXTRA HANDLES

Printing of extra handles to the product. This extra part can be handled for transportation or holding a postprocessing clamp (see Figure 2). The handle can be printed with small contacts to the products so it can be removed with minimum effort.

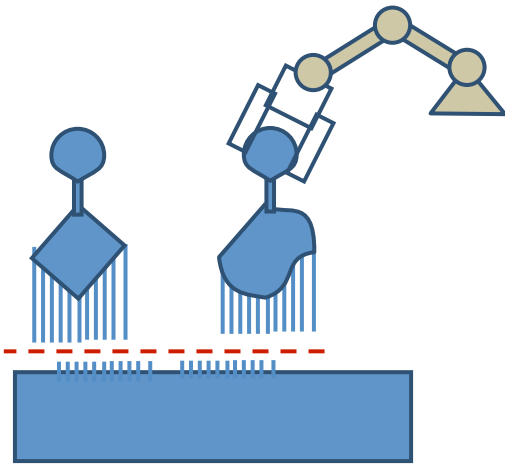


Figure 2: Concept with printing a extra handle to the product.

For the user cases the following handles have been designed (see Figure 3): For the hinge, the handle is a block on the side of the product. This enables to hold the product, and all the drilling and postprocessing can be done. After finishing, the block can be cut away by e.g. wire-EDM. For the mirror object the handle is under an angle, since the product must be printed under an angle because of the internal structure of the product. The current faces of the handle are now straight surfaces perpendicular to the layers of the 3D printer, to achieve the best position of the product.

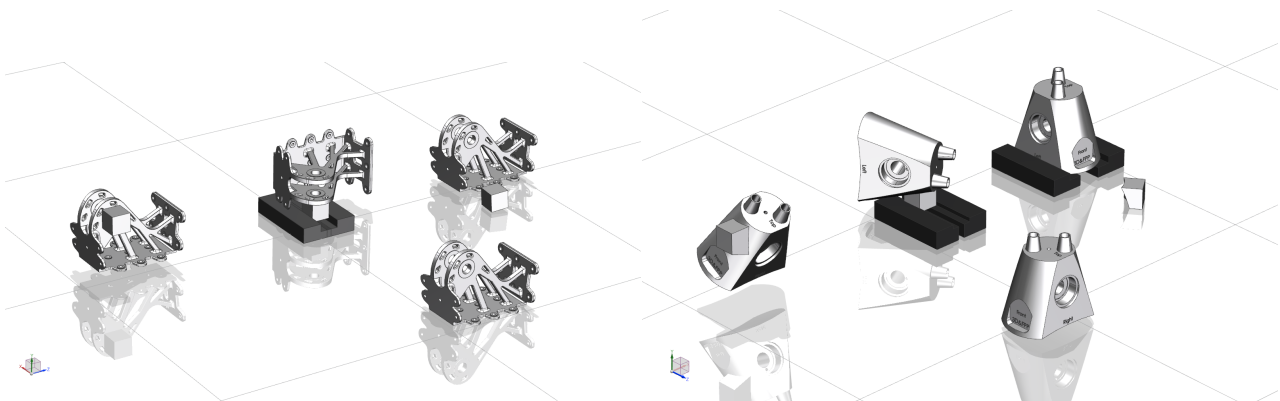


Figure 3: concept of handle to usecase products. Left: the Hinge, Right the mirror object.

For feasibility, the mirror object is chosen to test.

Aspects to test and verify on a milling machine:

- clamping stability
- tool accessibility
- stiffness
- ease of clamping / declamping

Aspects that are mentioned in the trade-off Table 1, like environment, coolant will not be tested because it is obvious.

To design the handle, finite element calculations are made to predict the stiffness, and vibrations. The handle is fixed to the mirror object with 8 rods of 3 mm diameter. These rods are easy to cut and remaining can be grinded away (see Figure 4).

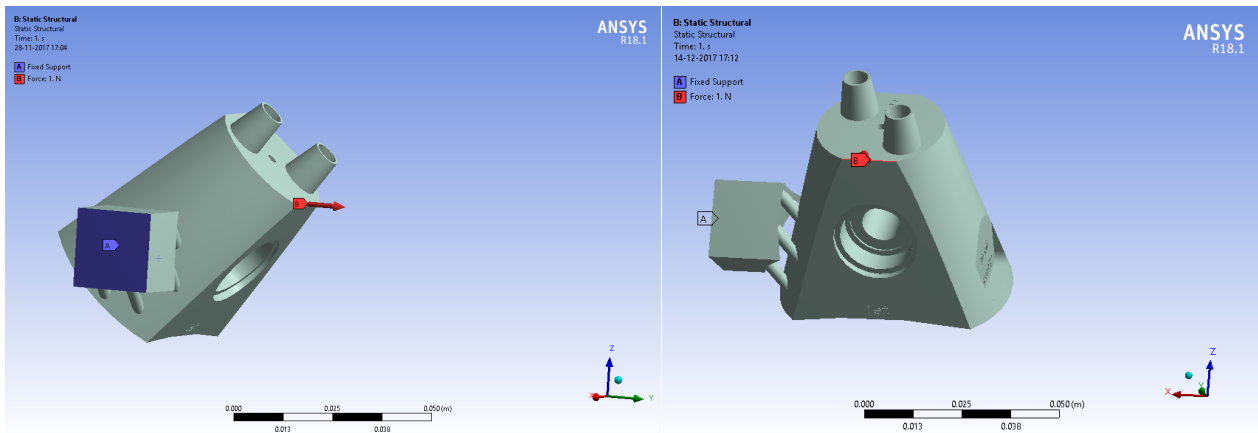


Figure 4: Model of mirror object with handle

For stiffness calculations and vibrations calculations, the handle is clamped. And a force of 1 N is applied (see Figure 5). The calculation is linear so the answer is scalable.

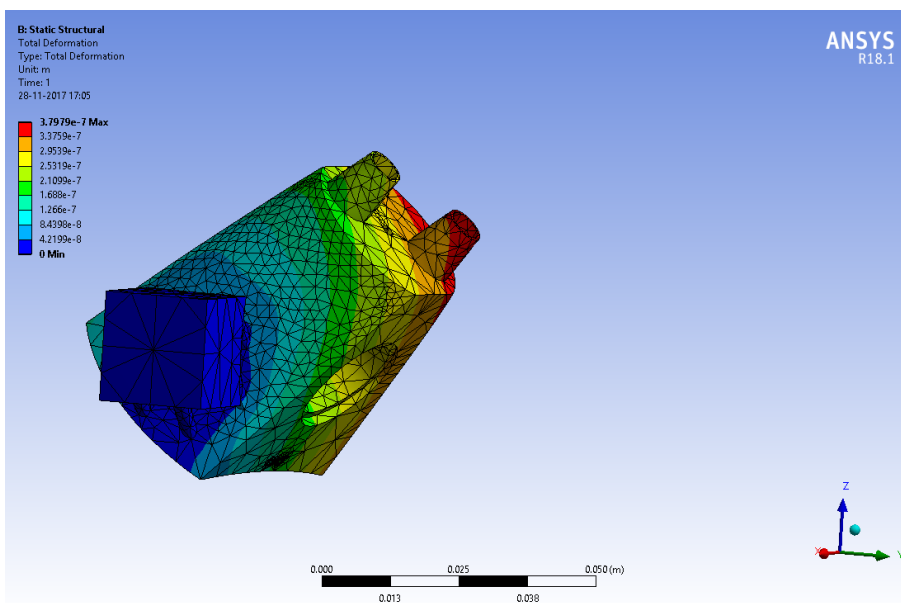


Figure 5: deformations due to 1 N force. The deformation is  $0.38\mu\text{m}$ .

The deformation of the product because of 1 N force is  $0.38\mu\text{m}$ . Therefore the stiffness is  $2.6 \cdot 10^6 \text{ N/m}$ . Which is on the low side. Increasing the thickness of the struts will not help. The position of the handle on the thin wall of the product is the main reason for the low stiffness.

The eigenfrequency is important to be able to cut the surface and vibrations cause scratches on surfaces, and noncompliant surfaces. The calculations show the first eigenfrequency of 889 Hz. Which seems high enough. The second mode is 953 Hz.



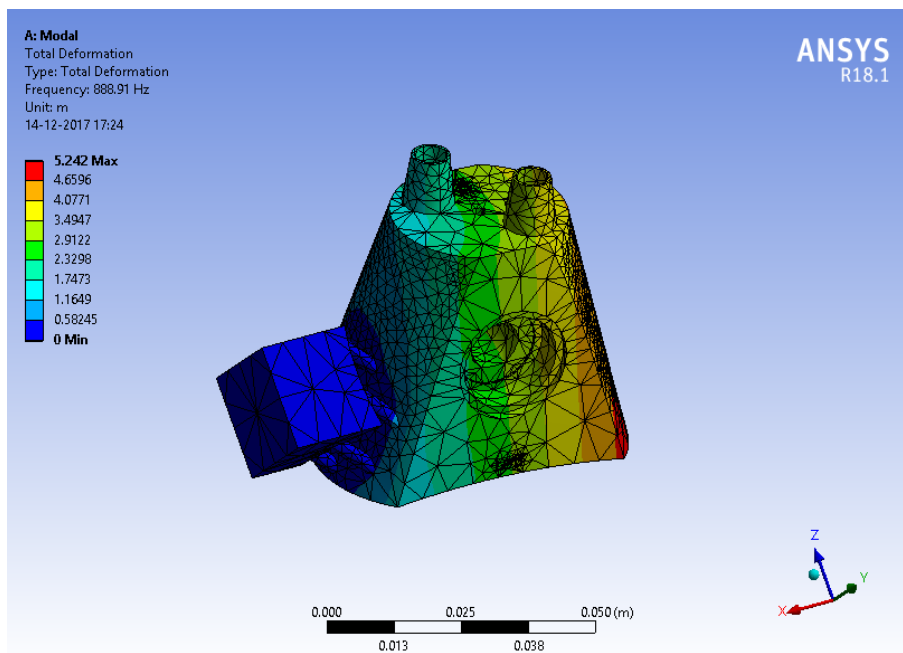


Figure 6: first eigenfrequency mode is 889Hz.

The samples are printed and are due to test. After the products tested, the results will be added to this document. The products are shown in . In Table 2 the advantages and disadvantages are given of using extra handles for clamping to the printed object.

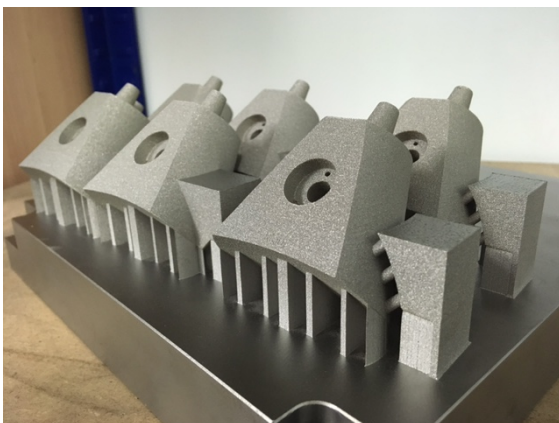


Figure 7: printed products on base plate. Before removing support structures



Figure 8: Left: mirror object without handle; middle:, Mirror object with handle and struts interface; right: mirror object with solid handle.

Table 2 Advantages and disadvantages extra handles.

Advantages	Disadvantages
Extra block with reference surfaces	Extra printing cost
Same material as product, compliant with machine environment/ cooling liquids.	Not all surfaces can be used.
Possible to standardisation	Designer must choose where to print handles to prevent low stiffness areas
	Design of struts also depend on orientation of product in print job.

### 3.1.2 CONCEPT 2: CLAMPING WITH HOTMELT

The use of hotmelts for clamping has a lot of aspects:

Chemical aspects:

- Apply to metal surface ( flat, and rough) – will it stick, what is the adhesion?
- Can it be cleaned? Can it be removed from the surface. Do you need solvents like water, IPA, Aceton or other to remove the hotmelt from the product. Or can it be mechanical removed ( with a knife). Maybe at elevated temperature?
- Is the clamp system resistant to e.g. coolant, which is used in workshop machines?

Mechanical aspects:

- Is the stiffness/ strength at room temperature good enough to clamp the products
- Is the hotmelt based on good adhesion, or for holding without adhesion
- Can the hotmelt be machined? What happens if the cutting tools touches the hotmelt. Does it create chips, or degradation the cutting tools
- It is stable at elevated temperatures

Process aspects:

- Temperature of applying, and must the product be at elevated temperature?
- Time of applying
- How much hotmelt to apply.

For the feasibility test we select 3 candidates:

- 3M™ Scotch-Weld™ Hot Melt Adhesive 3798 LM
- Thermelt814
- Supergrip (polyester urethane).

The 3M 3798LM is a low temperature fugitive glue meaning it can be easily removed without residual tack or residue. The 3798LM bonds to a wide variety of materials and applications that require a non-permanent bond. Generally, it is applied to marketing applications where one object (a sample, coupons, credit cards, etc.) is glued to another surface. Gummy Glue is also known as fugitive glue, credit card glue, e-z release glue, and some even call it booger glue.

According to the technical data (<https://multimedia.3m.com/mws/media/663330/hot-melt-adhesive-3798lm.pdf>), the recipe is as follows:

1. Hot Melt Adhesive 3798 LM must be applied with a 3M™ Scotch-Weld™ Hot Melt LT Applicator at 129°C. This applicator is designed exclusively for low-melt adhesives.
2. Apply to one surface. Make bond as soon as possible. Bond strength is maximized when open time is reduced.
3. After the bond is made, there is immediate strength and no clamping is necessary.
4. Optimum release on some substrates may require up to a 24 hour dwell time for clean removal.
5. Adhesive may bleed onto porous surfaces or cause staining. It is advisable to evaluate the adhesive on a test substrate for undesirable effect.

Thermelt814 is a polyamide hotmelt, which means it is a hard/stiff material.

Supergrip is a polyester urethane material, which has a strong adhesion.

#### 3.1.2.1 *Chemical aspects*

The adhesion is tested for the hotmelts using the Elcometer adhesion tester. In this tester an interface knob is “glued” with hotmelt to the 3x printed surface. By pulling the knob from this surface, the stress is measured. The stress can be measured upto 7 MPa. Based on the test also the residue of the hotmelt on the 3D printed can be found. In Table 3 the results are shown. The Thermelt has an adhesion of 7 MPa, but it leaves contamination on the surface. The Supergrip has a much lower adhesion and the surfaces are clean.



Figure 9: Elcometer Adhesion Tester.

Table 3: adhesion tests. The candidate materials( except for the 3798 LM) are tested, and also some other materials.

Material	3M 3798 LM	Thermelt 814	Supergrip 9850
Experiment	Not available yet during test		
Adhesion		7 MPa	2 MPa
Contamination		Hotmelt remains on sample	Hardly any hotmelt remains on sample
Stiffness		Though	Though
Material	Abifor 512	Shellac	
Experiment			
Adhesion	>7 MPa	3,5 MPa	
Contamination	NA	A lot of hotmelt remains on sample	
Stiffness	Though	Hard, very brittle	

### Cleaning of the sample

Thermelt814 does leave residue and with supergrip only limited residue. The 3M melt has been ordered and received, but no initial test performed.

#### 3.1.2.2 *Mechanical aspects*

To get an understanding of the effects of adhesion or Non-adhesion on the product, finite element calculations have been performed.

### Perfect Adhesion

For the test with high adhesion, the mirror block is mounted to a flat stiff surface. The thickness of the hot melt layer is 1-5 mm (see Figure 10). For material properties, the Youngs modulus of the hot melt is assumed 20 MPa and a nonlinear contact model is made, no time dependent plastic deformations are taken into account. The deformations are scalable with the force.

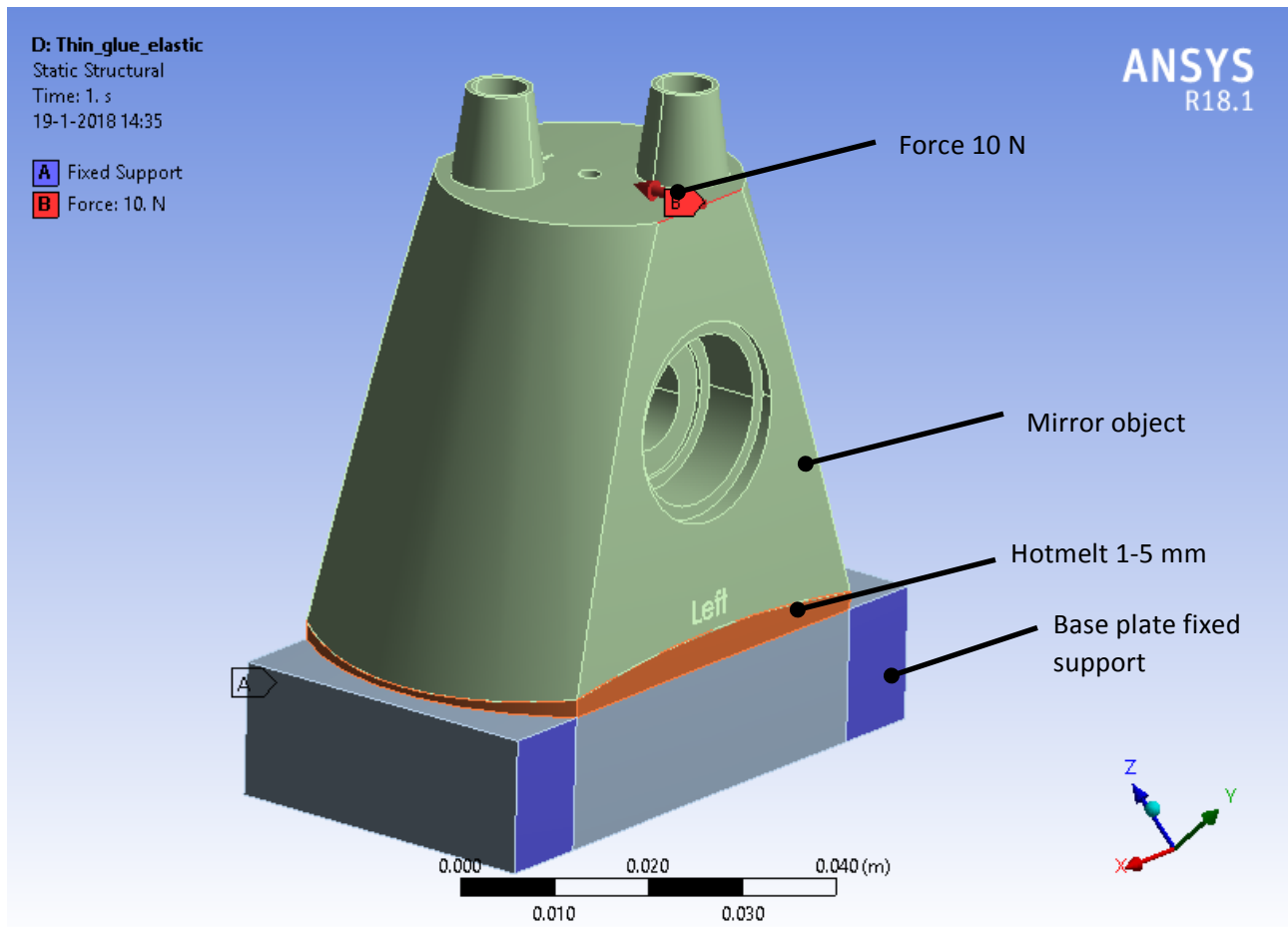


Figure 10: model of mirror object on a layer of hot melt

The deformation as a result of 10 N is 18  $\mu\text{m}$  (see Figure 11). This means that the stiffness is  $0.6 \cdot 10^6 \text{ N/m}$ , which is close to  $1 \cdot 10^6 \text{ N/m}$  which is minimal required. Since the model is linear in this scale, the deformation due to a 10x bigger force is also a 10x bigger deformation. This calculation shows that the Young's modulus of 20 MPa is too low. The minimum Young's modulus should be 2x higher. The numbers for Young's modulus are under investigation.

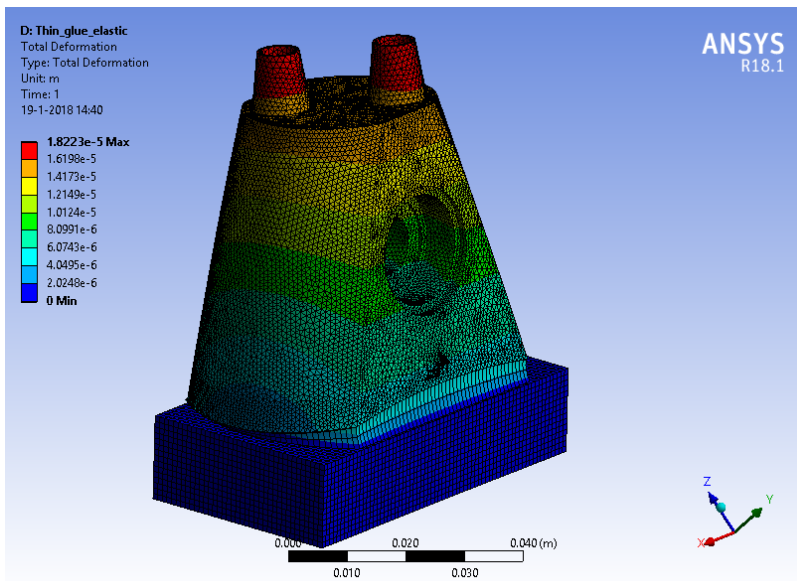


Figure 11: Deformations due to a force of 10 N

The adhesion forces in the contact can be calculated (see Figure 12). These values must be lower than the values measured in Table 3.

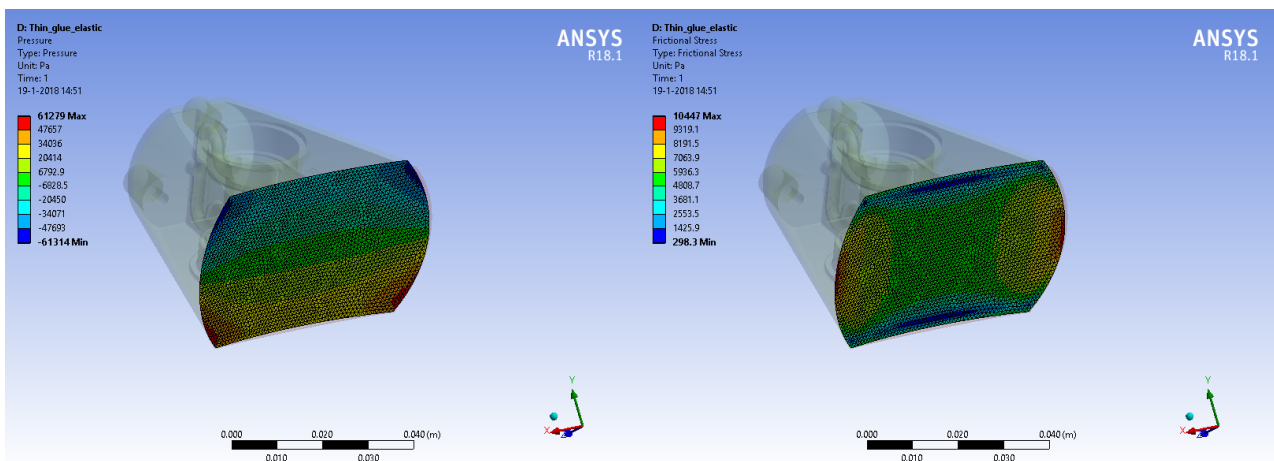


Figure 12: required adhesion forces for 10N force. Left the tension forces(0.06MPa) Right: shear force 0.01 MPa)

The required adhesion forces are much lower than the adhesion of the materials. Therefore the product will remain fixed during machining.

### No Adhesion/ clamping based on shape

For a concept of applying a shape inside a layer of hot melt, the model in Figure 13 is made. The Young's modulus chosen is 0.4 GPa. The force is 1 N, but to use rough sliding surfaces, this calculations is not linear anymore and also large deformations are in the model. This means that the result cannot be linear scaled.

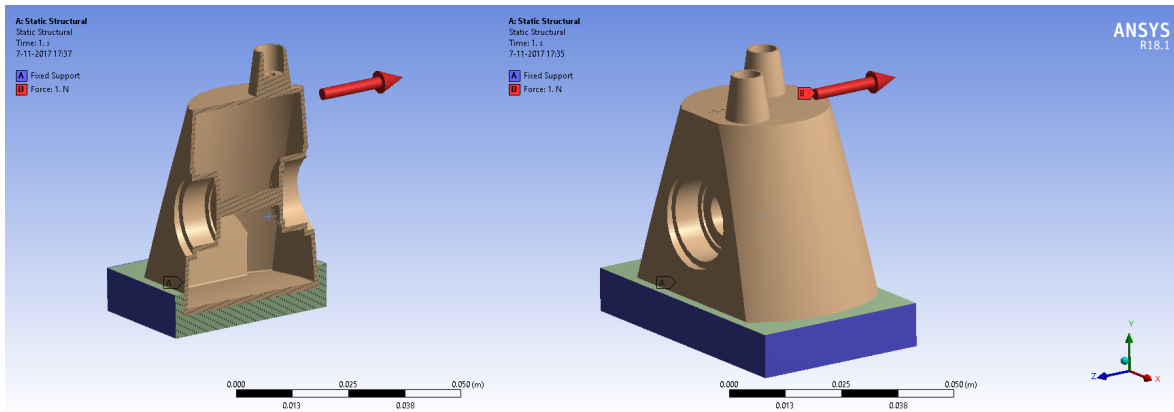


Figure 13: Model of mirror object in a bucket of material

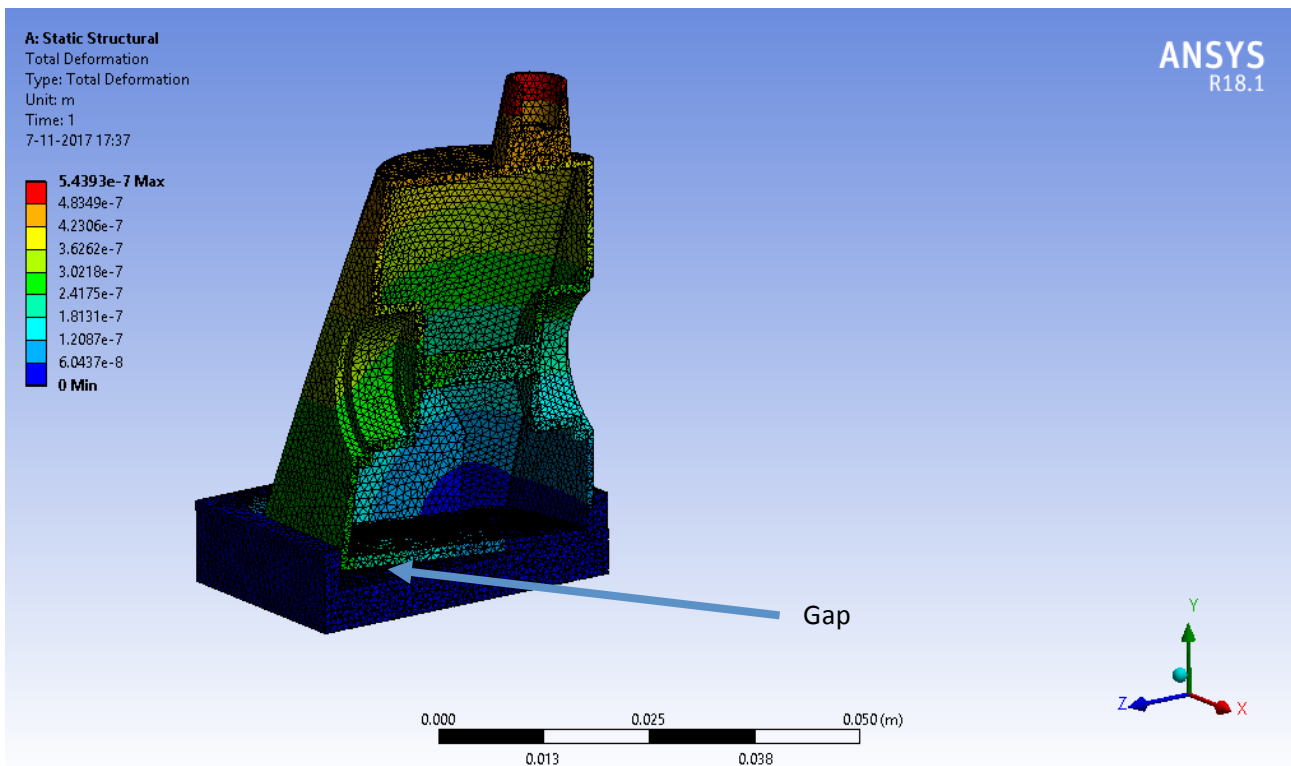


Figure 14: Deformations. Remind the deformations are scaled. The max movement is red and is  $0.5 \mu\text{m}$ . Sliding rough surfaces.

The models shows that the bottom of the mirror object will have no contact with the hot melt. Also because of the shape of the mirror object, the object can be pulled up. The total deformation is  $0.5 \mu\text{m}$  (see Figure 14), which result is  $2 \cdot 10^6 \text{ N/m}$  which is on the low end of the requirement.

Lowering the friction to 0.3, result in a stiffness of  $0.5 \cdot 10^6 \text{ N/m}$ .

Increasing the adhesion, as shown in Figure 15, result in a stiffness of  $15 \cdot 10^6 \text{ N/m}$

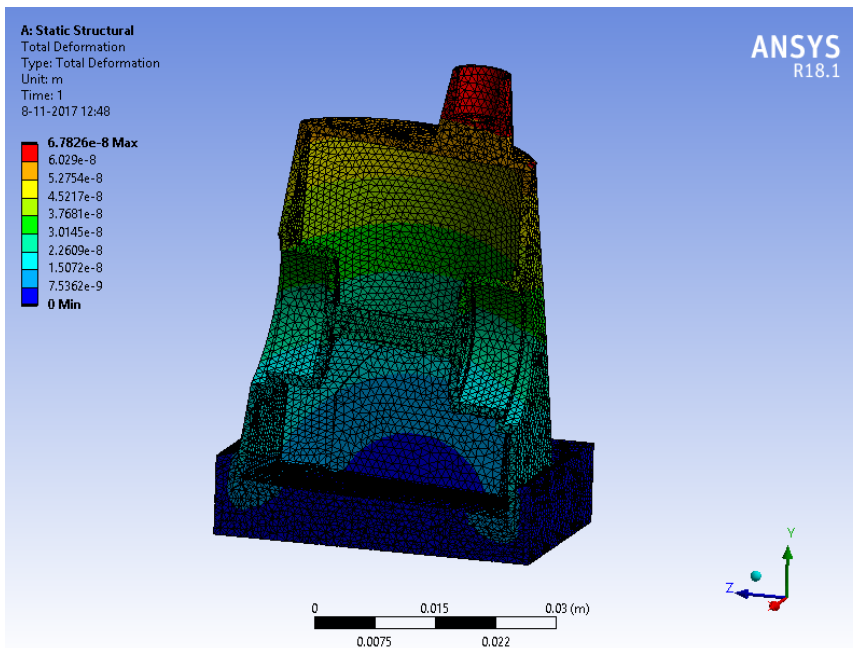


Figure 15: With high adhesion between the bottom of the mirror object, the deformation is 67 nm.

Conclusion: Clamping with a high adhesion is for clamping the best option. A low adhesion result in low stiffness, and if the adhesion is absent, the low Young's modulus result in release of the product.

Clamping with a Thermoplast (see Figure 16) is related to hotmelt, except for the application. It is assumed that the adhesion is low, and friction is low.

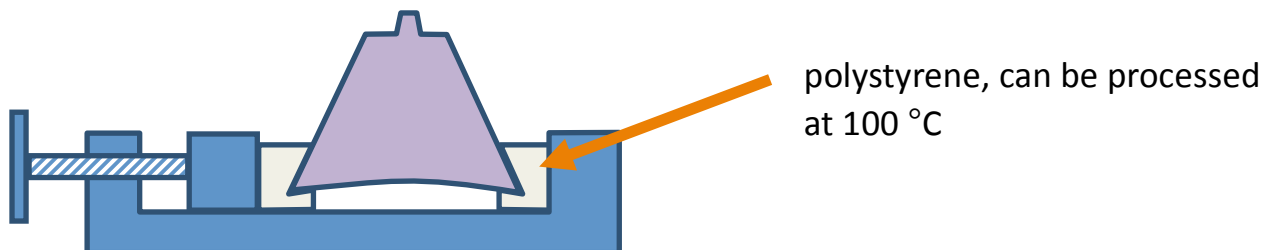


Figure 16: concept of clamping with a thermoplast

The advantage of Polystyrene is the low glass transition temperature of about  $T_g = 373 \text{ K}$  ( $100^\circ\text{C}$ ) and a high Young's Modulus of 2.28-3.28 GPa. It has a medium to high tensile strength (35 - 55 MPa) but a low impact strength (15 - 20 J/m).

The mirror object is hard to clamp with the concept above. The round shape result in rotation and with 1 N force the deformation is  $18 \mu\text{m}$  (see Figure 17). In the model no contact force is used, maybe this will lower the deformation.



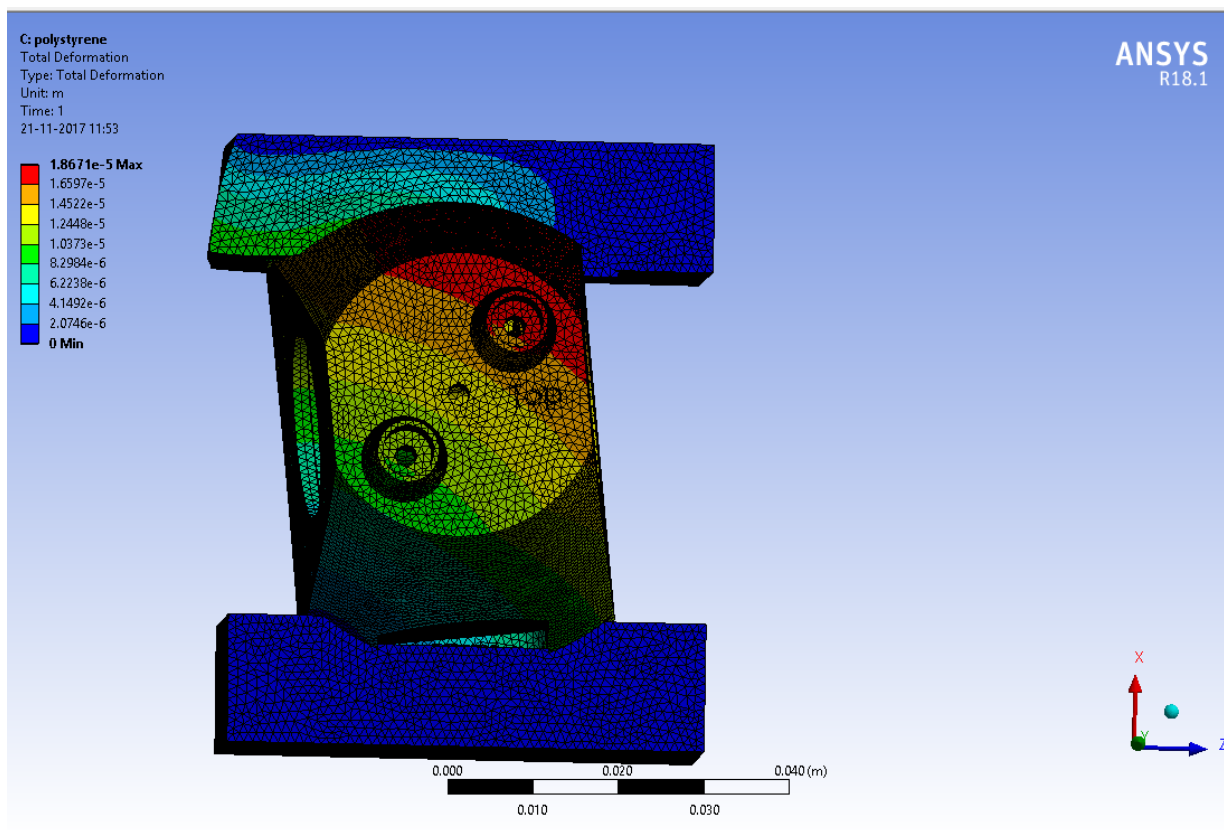


Figure 17: Result clamping simulation using a thermoplast clamp

The numbers for Young's modulus are estimated within the calculations. To get a number, some of the hotmelts have been tested using an Anton Paar MCR301 Rheometer. Figure 18: Anton Paar MCR301 Rheometer. In such a tool, two plates with the material in between get an amplitude sweep at 1 Hz and measures the shear modulus. The experiment is performed at isothermic conditions at 23°C.



Figure 18: Anton Paar MCR301 Rheometer

Table 4: mechanical material property

Material	3M 3798 LM	Thermelt 814	Supergrip 9850	Arbifor 512	Shellac
Feeling	Soft, elastic	Less hard, though	Less hard, though	Hard, though	Very hard, very brittle
$G'$ = storage modulus	4.7 MPa	7.4 Mpa		8.3 MPa	8.9 MPa
$G''$ = loss modulus	0.56 MPa	0.24 MPa		0.14 MPa	0.11 MPa
$ \eta $ *= complex viscosity	0.7 MPa.s	1.2 MPa.s		1.3 MPa.s	1.4 MPa.s
E (Calculated youngs Modulus assume $\nu=0.3$ )	12MPa	19		21.5MPa	23

The Youngs modulus in Table 4 are calculated by calculation the Shear modulus from the storage modulus and the loss modulus, and then assuming a poisons ratio and then the E modulus can be calculated:

$$G := \sqrt{G'^2 + G''^2} \quad \text{and} \quad E := 2 \cdot G \cdot (1 + \nu)$$

With these low Youngs Modulus the use of thick hotmelt layers must be omitted.

In Table 5 the advantages and disadvantages are given of using hotmelts for clamping printed objects.

Table 5: Advantages and disadvantages of hotmelts

Advantages	Disadvantages
Freedom in holding	Most clamping method are based on mechanical clamping. Acceptation of hotmelt will be a long path to accept.
Low cost clamping	Cleaning of the part
The right Hotmelt don't leave residue	Low Young's modulus.
	Without adhesion large deformations due to slip and low Youngs modulus.

### 3.1.3 CONCEPT 3: SOFTCLAMP BASED ON BED OF PINS

The standard method of soft clamping consist of a counter part of the product. To obtain high accuracy and stiff clamping, these counter parts must clamp the product uniform. Therefor these parts must be conformal to the product and fit perfectly. This is almost impossible for 3d printed parts that have high uncertainty on the dimension.

An adjustable softclamp based on pins, can take care of these uncertainties. Research brought us to the company Matrix Innovations, who have a commercial product available delivering this functionality. The clamp principle is shown in Figure 19:



Figure 19: Bed of pins clamp by [www.matrix-innovations.com](http://www.matrix-innovations.com)

In this set-up each pin is spring loaded. When all these pins are released, via one central clamp, a product can be positioned between 2 clamping blocks (preferably on a bottom-plane/reference such that the product is supported in Z-direction) and the 2 clamping blocks can be shifted towards each other. When the product is touched each pin will shift in the clamp with a given pretension. Once the product is enclosed by sufficient pins, all pins can be blocked with the central clamp and the product is fully locked in position. In Figure 20 you can see a test result with an available demonstrator (with 6mm pins). A part of the product is however covered with the clamping tool and cannot be milled. Also a test was performed with only one clamp (see Figure 21)

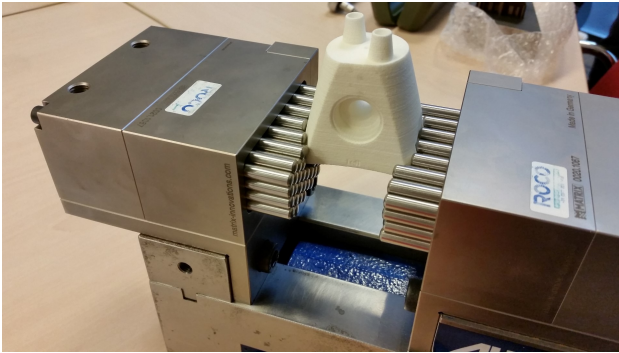


Figure 20: Matrix-innovation clamp with (polymer) user case of the mirrorblock

On the website one can see several video's of their applications. It is also possible to configure a robot gripper with this clamp to transport products between processing stations.

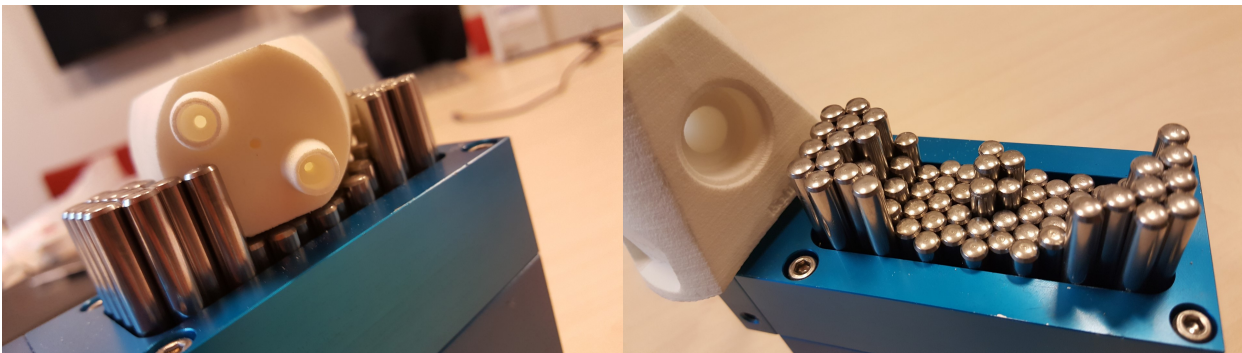


Figure 21: clamping a product with only 1 clamp. After fixing the pins, the shape of the product is visible and the product can be placed back again

### **Issues to expect:**

The bed of pins system is useful for odd shaped products. The clamping of regular shaped parts can be a challenge. Clamping of round products, can result in sliding of the product. And rectangular objects can also move and slide if clamped incorrect. The best way of clamping a rectangular object is rotated. This result also in repeatable reclamping since the product is automatically repositioned. The plastic hollow gearbox model is not stiff enough to clamp and show deformation (see Figure 22).



*Figure 22 clamping rectangular under an angle*

Since the bed consist of individual pins, single pins can also be used to support the bottom and not for clamping. A very versatile concept.

The system has an optional self-cleaning system to prevent cutting chips to slip into the tool.

TNO obtained a set. This set has 3mm pins and therefor better to hold smaller products. The pictures above are made with a part with 6 mm diameter pins.

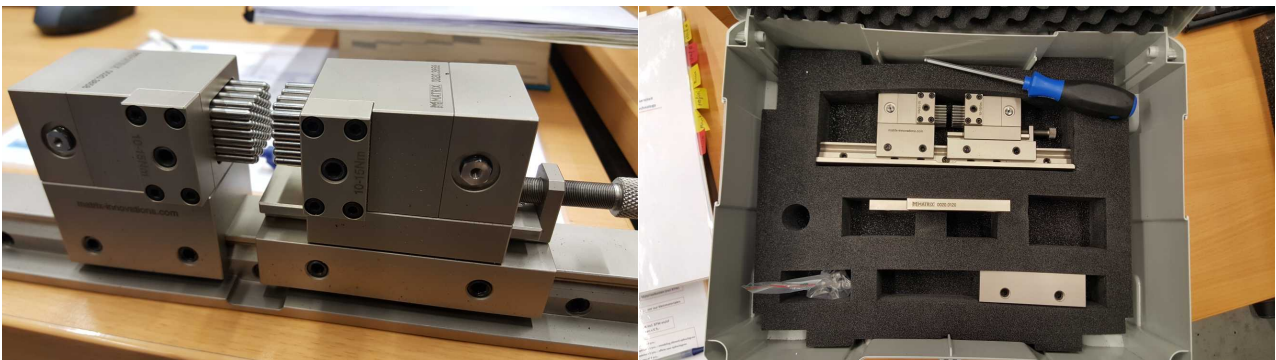


*Figure 23:Matrix innovation clamp bought by TNO*

In the near future the clamp will be used to machine a 3d printed mirror object.



Table 6 Advantages and disadvantages Bed of pins.

Advantages	Disadvantages
Reusable clamping concept	Slip with rectangular or round objects
1 <sup>st</sup> clamping and 2 <sup>nd</sup> clamping	Not all surfaces can be used.
Very good for odd shape products	Designer must choose where to print handles to prevent low stiffness areas
Reproducible re-clamping < 0.02 mm	
Self-cleaning system	

### 3.1.4 CONCEPT 4: PRINTING ON AN EXTRA BASE PLATE

At a demonstration meeting at Sirris (<http://www.sirris.be/nl/agenda/inauguratie-demonstrator-van-am-integrated-factory>), a clamping method of printing on a separate base plate is presented. A small block is screwed to the baseplate of the 3D printer. After printing, this small block is the interface for further post processing.

In the figure below, the concept that came up in brainstorming at TNO and Hittech is presented. This is comparable to the Sirris concept.

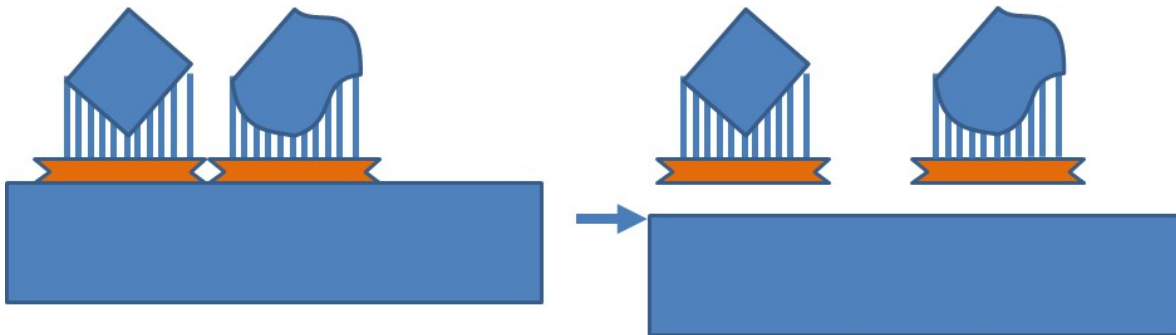


Figure 24: variation on baseplate concept / printing on standard clampplate

In the sirris concept, the product base plates will be mounted with screws to the baseplate of the 3d printer (see Figure 25). To enable a flat starting surface, the top is flattened by milling.

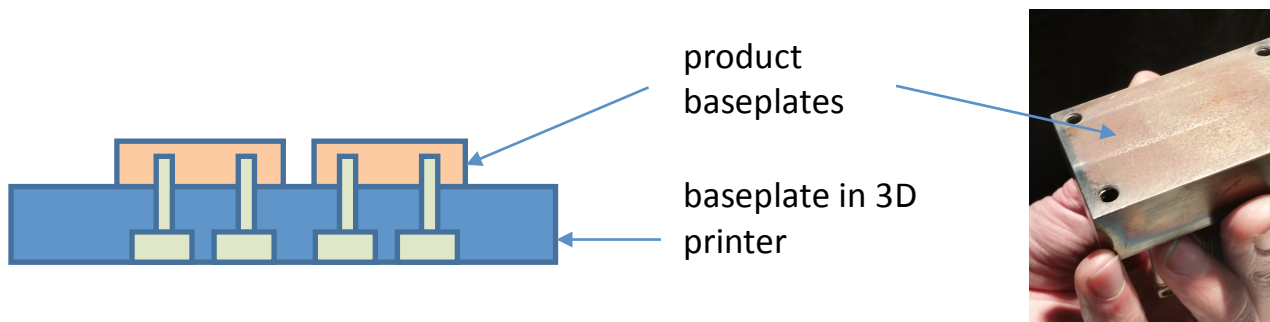


Figure 25: product plate is fixed by screws to the base plate.

The product will be printed on the product baseplates. Although the 3d printed product is rather thin and flat, the total printjob is large because of the support structures required for the clearance in the postprocessing machines. The positions of the product baseplates are not very accurate. Therefore reference planes are added, which can be used for alignment in the postprocessing machines.

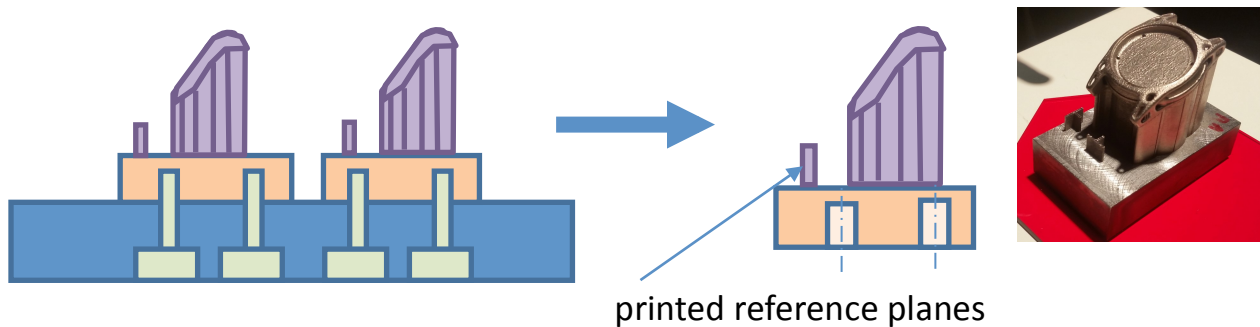


Figure 26: with printing of the product, also reference planes are printed for easy alignment with postprocessing

Table 7 Advantages and disadvantages extra baseplate.

Advantages	Disadvantages
Position accuracy of 3D printer is used for printing reference planes	Require higher printing supports, to create clearance for 5axis milling machine
No position scanning measurement is needed	Only possible for 1 <sup>st</sup> clamping step.
Only a second clamping tool is required, which can use reference surfaced made with the 1st postprocessing step.	Prepair and develop required extra baseplates
Most of the support structures can be milled away.	Optimum orientation for 3D printing is often not the optimum orientation for post processing.
No wire EDM required to remove product from baseplate	

The preferred solution to proceed with is the special interface printed on the product and/or in combination with the softclamp based on a bed of fins.

## 3.2 SCANNING

To validate the technologies for 3D scanning the most important aspect is the accuracy and repeatability of a technology. Once the accuracy is validated other aspects as the automation potential and the versatility of the technologies can be evaluated.

Based on the trade-off tables the 3D structured light technology was identified as the most promising technology and therefor this technology was selected for the main feasibility study. The other 2 technologies were also investigated but in less detail.

### 3.2.1 ACCURACY & REPEATABILITY

Based on the user cases a general accuracy of  $\pm 0.01$  mm to  $\pm 0.03$  mm was required to quantify the 3D shape of the parts. The more accurate dimensions from the 2D drawing were put outside of the scope of the exercise since they are only present in the final post-processed part and other more accurate technologies are available for the final quality check. The mirror object user case (see Figure 27) was used for the validation of the accuracy and repeatability.

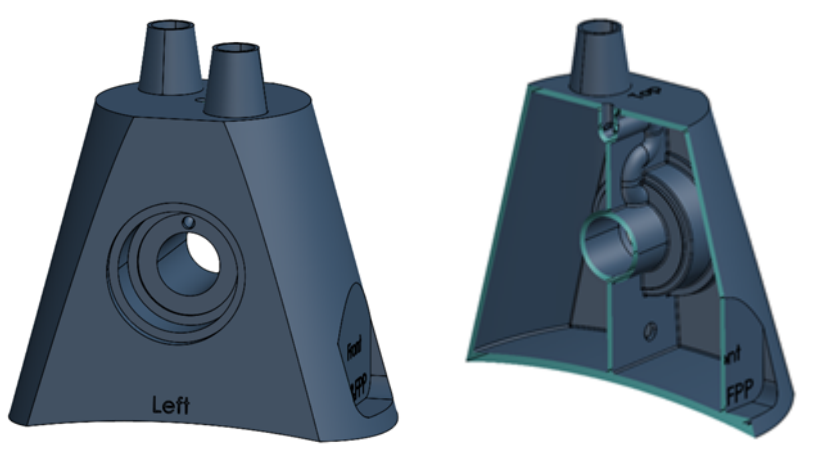


Figure 27: user case: mirror object

The following hardware system was used to scan the object:

- GOM ScanBox 5120
- ATOS TripleScan III 16 MP with 560 mm measuring volume

The measuring volume of a 3D scanner refers to the set of lenses which is used in order to illuminate and scan the object of interest. Since the resolution of a particular 3D scanner is fixed, lowering the measuring volume results in higher accuracy and vice versa. The 560 mm measuring volume is a good all-round volume for medium sized parts in the automotive sector. Since the 3DFPP mirror object is quite small, a smaller measuring volume would probably be a better choice. However, Argon opted for the 560 mm volume because this has a higher flexibility potential for future automation since all parts < 560 mm LxWxH can be contained completely in the measurement volume.



The 3DFPP Mirror Object was scanned multiple times consecutively. In order to take into account and to differentiate between the influence of both the scanning variation (exact setup) and the variation of alignment (same product but different setup) calculation, the first scan sequence was made with an identical setup and for the second scan sequence the part was moved in between the scans to create a new setup each time.

For the first sequence the repeatability was  $< 0.01$  mm and this increased to  $< 0.03$  mm for the second measurement sequence identifying the influence of part positioning in the measurement system. Below the overview is given for the second scan batch. The colours represent the deviations between the different measurements. A range of 0.03 means that all deviations between the measurements are within the interval of  $[-0.015$  and  $+0.015$  mm].

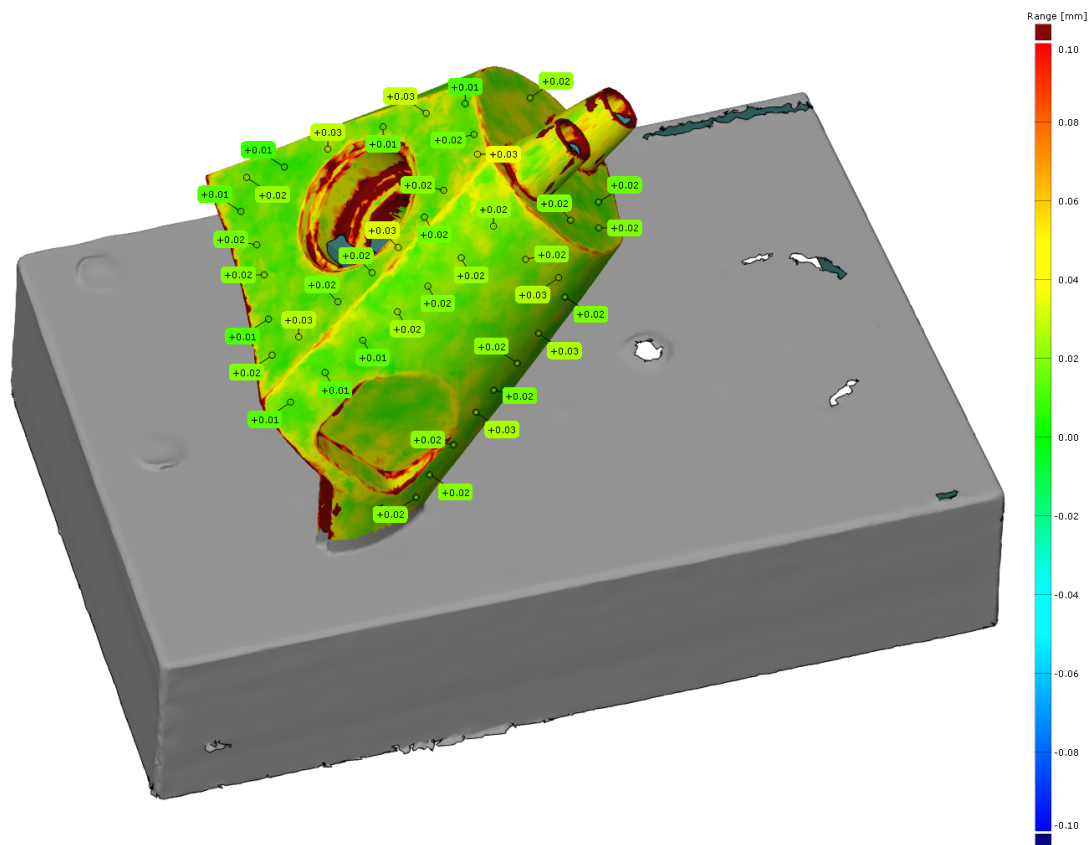


Figure 28: measurement repeatability between 10 measurements

Based on these results the 3D structured light technology with the GOM hardware was validated for the project scope of the 3D&FPP project.

### 3.2.2 AUTOMATION POTENTIAL

The GOM hardware provides also a software package, ATOS professional, which has integrated modules to allow automated, robotized measurements (VMR license), analyse the 3D measurement data (Inspect license) and to automate custom defined workflows (Python environment). The combination of this software with the versatile hardware (16 Megapixel camera which allows larger measurement volumes for the same accuracy) makes that this technology very well suited for the required automation and TRL specifications of the 3D&FPP project.

### 3.2.3 PROCESSING 3D DATA FOR MILLING MACHINE COMPENSATION

Once the technology accuracy is validated the next step is to check if it is possible to deliver the required output for the CAD/CAM process step. This is required to relate the object's position and orientation to the coordinate system of the milling machine and can be represented by a 4x4 transformation matrix.

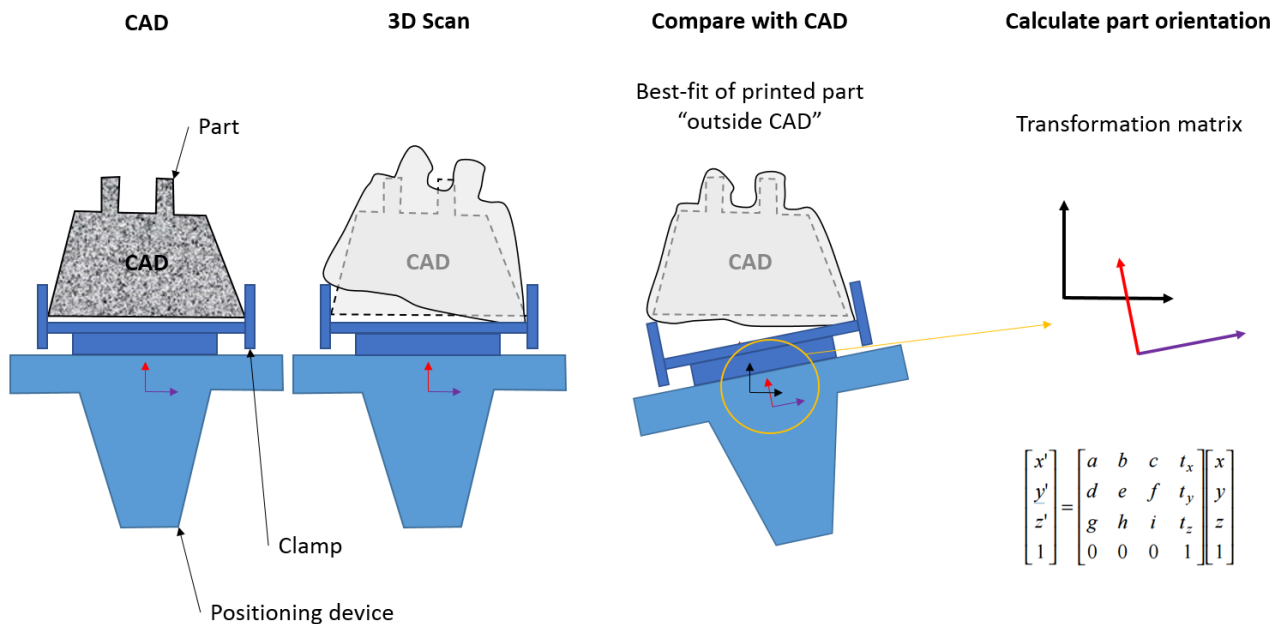


Figure 29: schematic explanation of the matrix computation

For the first test the same mirror object was used and clamped to simulate the interface of the positioning device. By using the same female recipient during the scanning and milling this can be used as the reference for the positioning and the 4x4 matrix can be calculated.

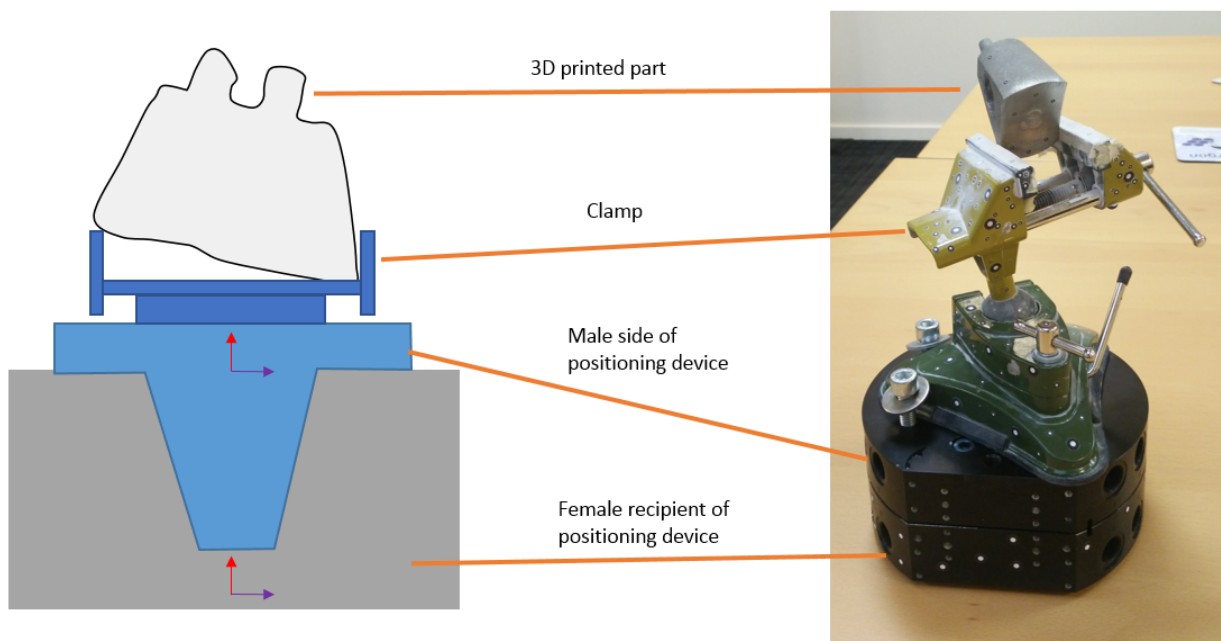


Figure 30: test setup

The mirror object was scanned 5 times in a different clamp orientation and afterwards processed in the GOM software to calculate the corresponding transformation matrices.

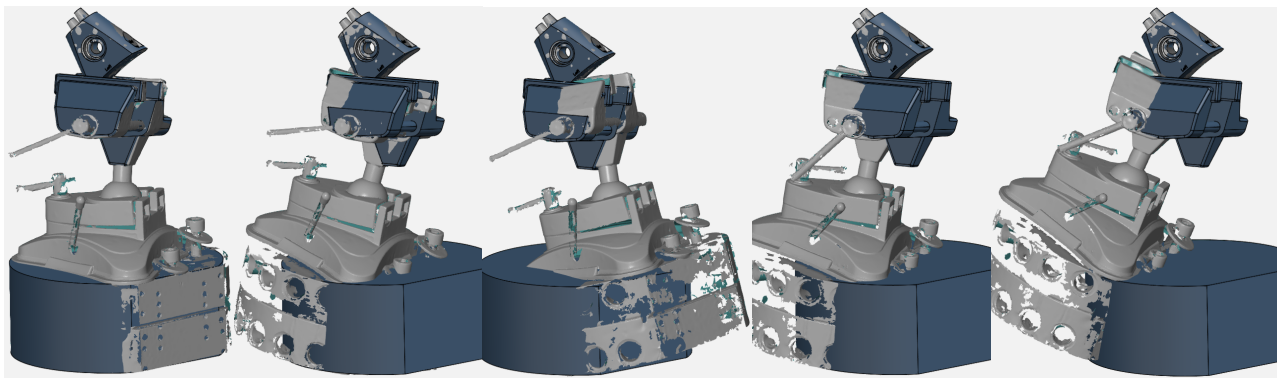
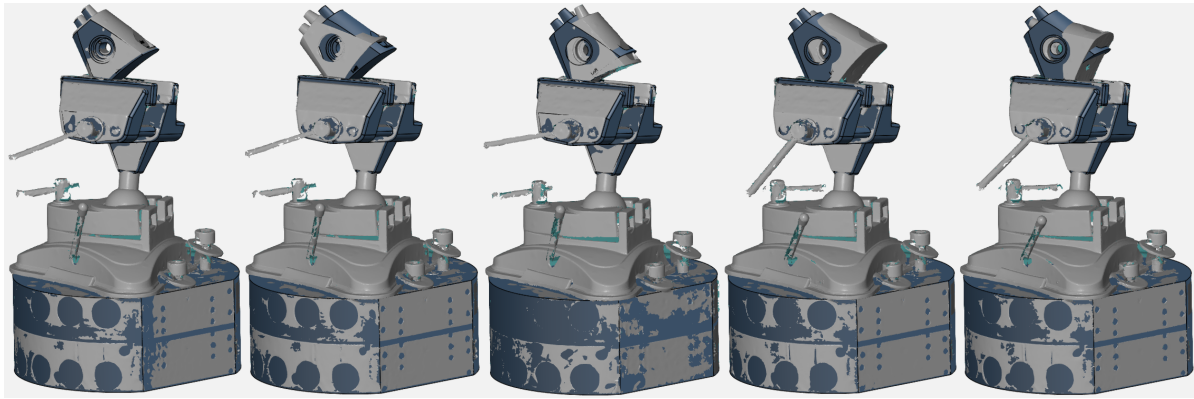


Figure 31: orientation compensation and transformation matrix calculation

An example of the transformation matrix for scan 2 is shown below:

$$T_{scan\ 2} = \begin{bmatrix} 0.99 & 0.05 & 0.10 & -22.12 \\ -0.03 & 0.98 & -0.19 & 44.59 \\ -0.10 & 0.18 & 0.98 & 4.94 \\ 0 & 0 & 0 & 1 \end{bmatrix}$$

This matrix can be decomposed in a rotation component and a translation component:

$$Rotation_{scan\ 2} = \begin{bmatrix} 0.99 & 0.05 & 0.10 \\ -0.03 & 0.98 & -0.19 \\ -0.10 & 0.18 & 0.98 \end{bmatrix} \quad Translation_{scan\ 2} = \begin{bmatrix} -22.12 \\ 44.59 \\ 4.94 \end{bmatrix}$$

In collaboration with Hittech a second test has been performed where a part was milled on a CNC machine and afterwards scanned at Argon. The milled part was designed to have a flat top surface with a specific angle so that it was not horizontal. The goal of the exercise was to calculate the required rotation angles for the milling machine table to position the part so that with these rotations the milled plane would be positioned perfectly horizontal in the machine.

After the calculated angles were applied in the milling machine some deviations were observed and the plane was not perfectly horizontal. After further investigation this led to the observation that the rotation axis of the milling machine were not perfectly aligned with the calculated model and that the rotations are

converted in the software of the milling machine to compensate this internally. This could mean that each machine has a unique compensation code which has to be determined each time in order to use this technique. Further tests are necessary to clarify the consequences of this finding.

Our algorithms compute the necessary rotation about Y and Z axis so that the normal of the milling plane equals the global Z – axis.

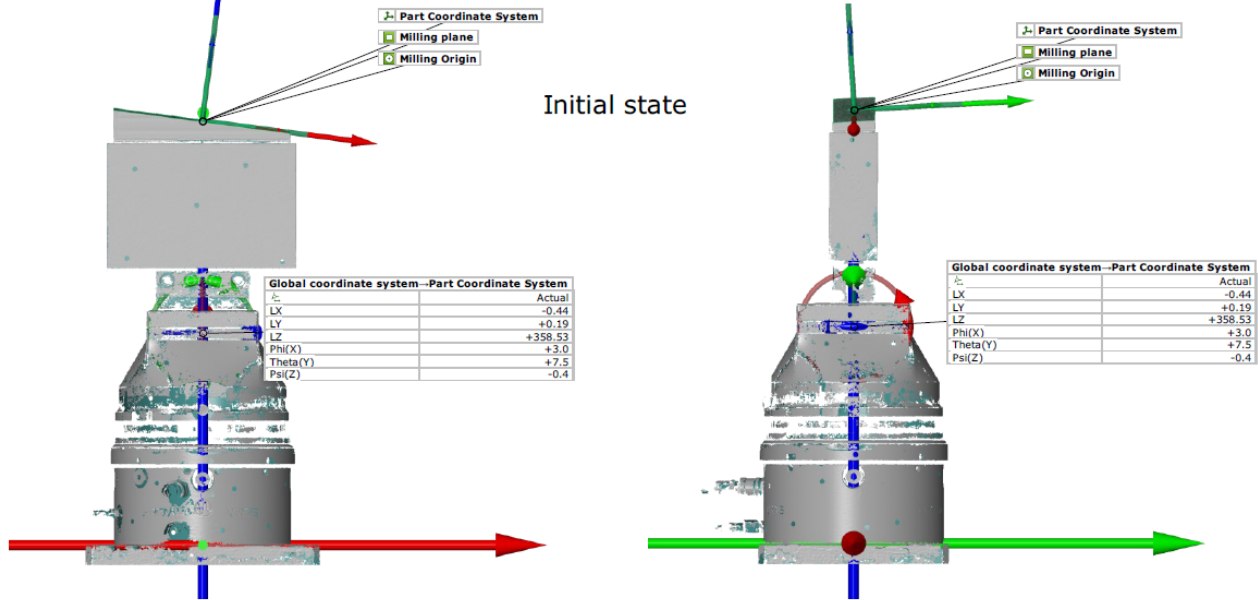


Figure 32: initial state – top plane of is not horizontal

#### Alignment: Corrected Alignment

Our algorithms compute the necessary rotation about Y and Z axis so that the normal of the milling plane equals the global Z – axis.

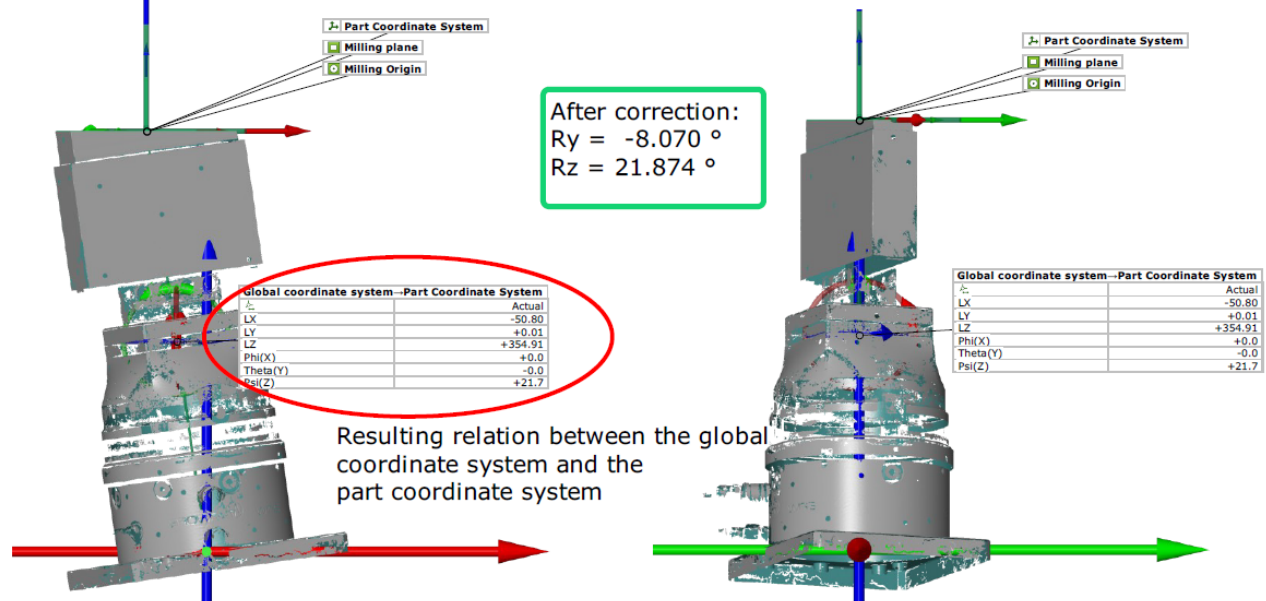


Figure 33: After compensation – top plane is horizontal.

### 3.2.4 FUTURE TESTS

The tests described above were all performed on the option to immediately alter the milling machine orientation based on the 3D scanned data and keeping the original CAD/CAM algorithms. With the current finding that this compensation would be different for each machine the other option where the CAD/CAM algorithms are altered could be a better generic solution. These tests will be performed in collaboration with the UoE.

## 3.3 POLISHING

In the post polish test plan, written by Hittech Multin, a mathematical overall tolerance calculation of surface roughness and material removal caused by various subsequently applied production techniques was postulated.

Based on these derived formulas it was calculated that a certain order of production treatments in conjunction with 3D printing could or could not achieve certain surface roughness and geometry tolerance levels.

For proof of principle purposes multiple samples of different materials and geometry are prepared and measured for their initial geometry and roughness.

After treatment of the samples their geometry and roughness will be measured and set against the postulated outcome.

The outline of the first test of these samples with a domeless rotary vibrator is described in the following paragraph.

### 3.3.1 TEST DOMELESS ROTARY VIBRATOR

The working principle of the domeless rotary vibrator (DRV) technique is having chips grind over the to be polished surface. The movement of the chips is randomized. Since it concerns a lot of chips, material is removed slowly from the surface and the products are exposed for a long time. In theory the result is to some extent reproducible.

The goal of this test is find out how reproducible the DRV technique exactly is. Up until now, there are no specifications on the quality level of this process and therefore the results of this test are important to determine how suitable the DRV technique is. Preferably, the test is set-up such that its results apply to the large variety of products and geometries that one encounters with 3d printed products. With this intent, different geometries and materials will be tested. It is important to test different shapes because the performance of this specific technique is correlated to the geometry of the product.

In this section the design of the test assembly will be presented and it is discussed which surface measurements are done before the test assembly is polished. The first results of this polishing test are expected the end of January.

#### Design of test assembly

In Figure 35, an overview is presented of the complete test assembly. Note the circular hole cut-out in the middle of the base plate. This base plate is attached to the stationary bed of the rotary vibrator by bolting it

on the bed via a threaded rod which goes through the last mentioned hole in the base plate. In figure 23 the threaded bolt is denoted which is referred to.

Different objects are attached to the base plate to determine the performance of the polishing process in different cases. Each object will be discussed separately in the following.

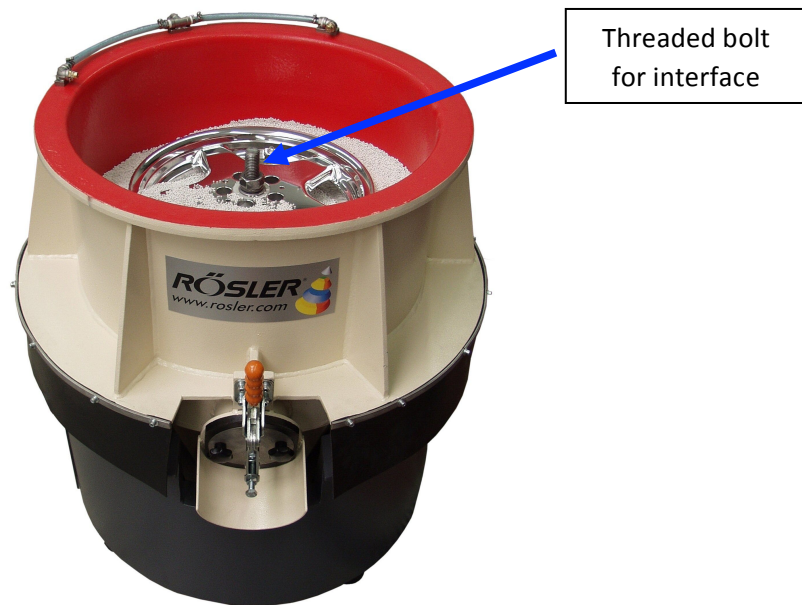


Figure 34 - In this figure the threaded rod and bolt are denoted which are used to clamp the product to the stationary bed of the machine.

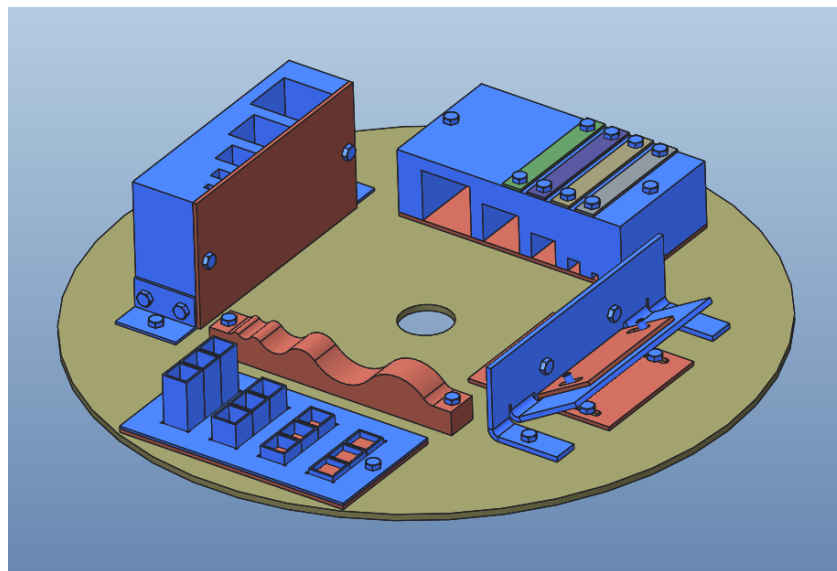


Figure 35 -Overview of the complete test assembly.



## Testing cavities of different depths

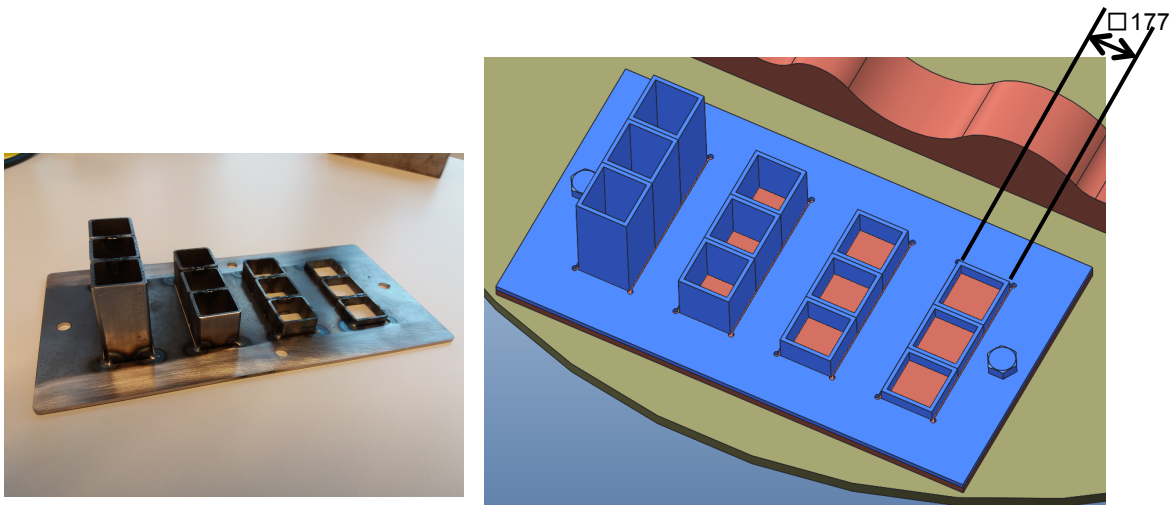


Figure 36 –assy to test the performance when polishing cavities. The red plate is the actual sample that is measured. The blue weld-assy simulates the cavities in a product.

With the DRV technique it is possible to polish inside cavities. However, the result is probably affected by the depth of the cavity. A weld-assy is designed to simulate the cavities in a product, this weld assy is depicted in Figure 36. This weld-assy is attached on top of the sample that will be analysed, depicted in red in Figure 36. Four depths are measured (40, 20, 10 and 5 mm) and per depth three measurements are done. The expected results after polishing is that the surface of test samples at the deeper cavities will be rougher with respect to the surface at the shallow cavities, thus less material is removed from the surface in deeper cavities.

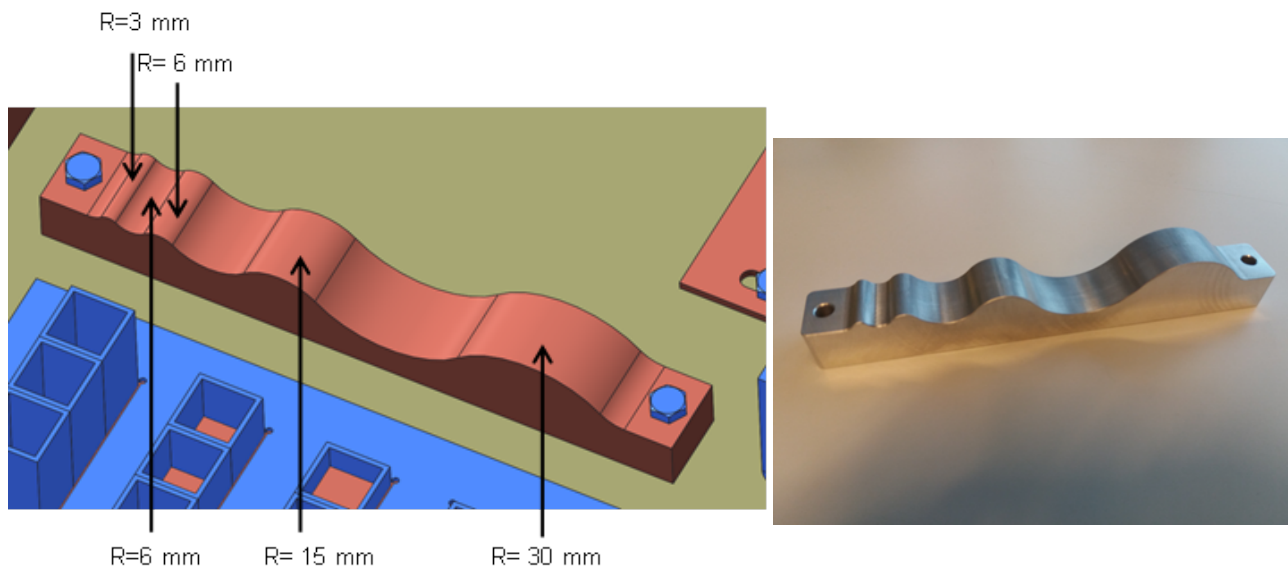
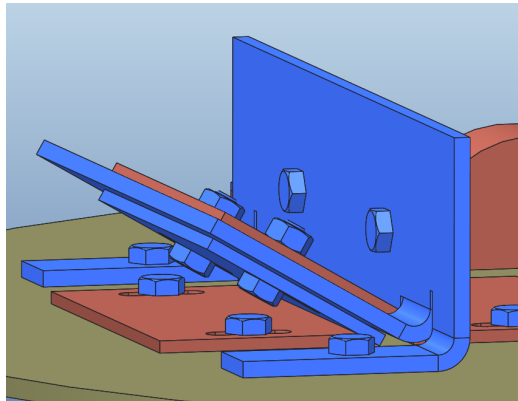
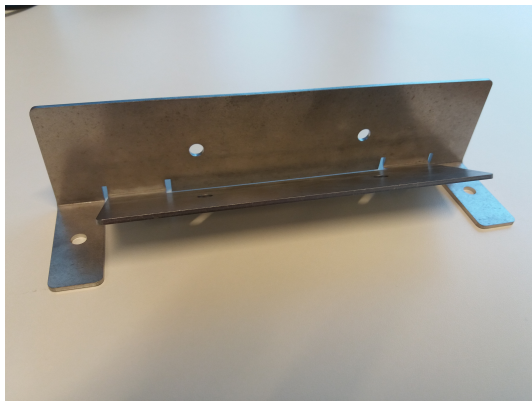


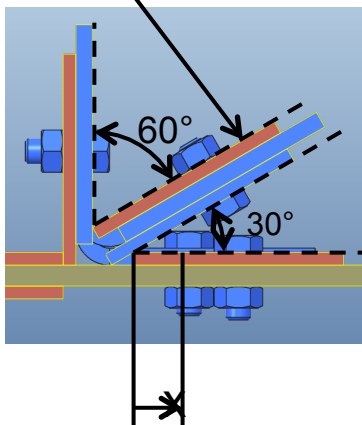
Figure 37 - Test sample to compare the polishing result for products with differently curved surfaces

### *Different curvatures*

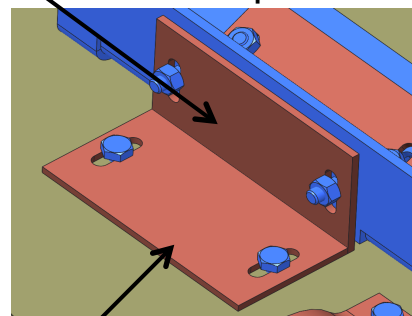
In Figure 38, the test sample is depicted that is used to test whether there is a relation between the polishing result and how much a product is curved. It is expected that more material is removed when the sample is more convex. And vice versa, that less material is removed when the surface is more concave.



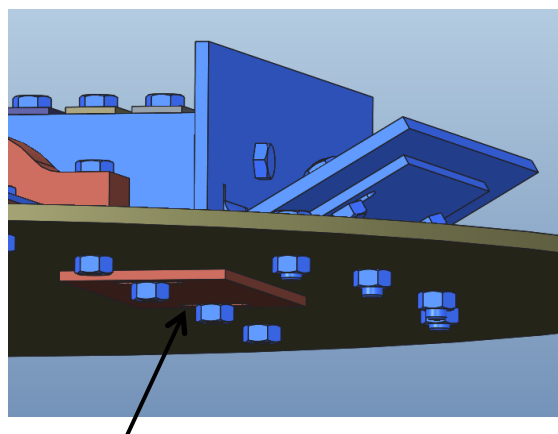
Orientation of plate is  $30^\circ$



Orientation of plate is  $90^\circ$



Angle between plates is  $90^\circ$



Upside down orientation

Figure 38- Resulting roughness is measured as a function of x



## Orientation and angles

Presumably the orientation of the product will also affect the result and some corners are not reachable by the chips. In these part of the test the plate are positions in different angles and the roughness is measured as a function of  $x$  as illustrated in Figure 38. Around  $x=0$  the roughness will not be reduced, it is interesting to find out from which distance the roughness will begin to decrease and how this is related to the geometry of the chips.

## Materials and internal channels of different sizes

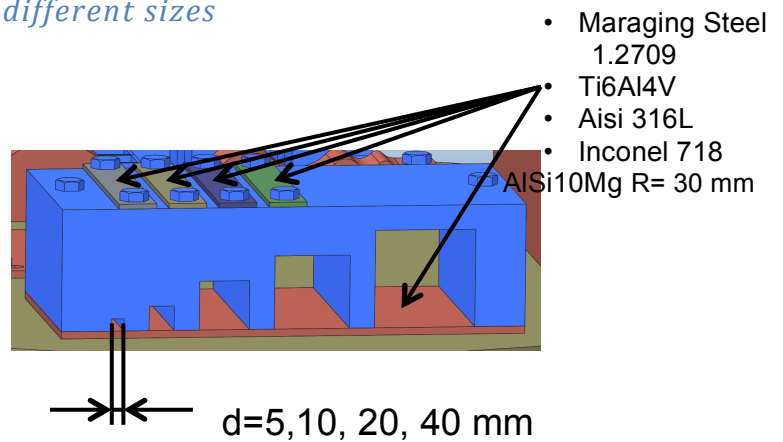
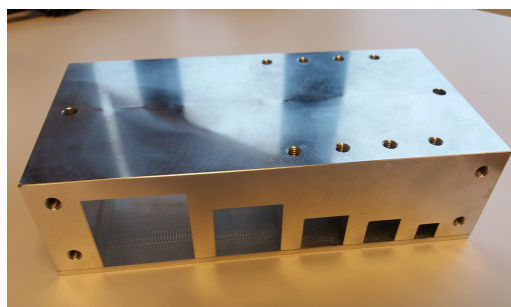


Figure 39 - Set-up to investigate difference when polishing different materials and analyse how well internal channels can be polished.

All previously introduced samples are made of aluminium. In the set-up presented in Figure 39, four plates of different materials are mounted on a block. Probably there exists a correlation between the hardness and strength of the sample with respect to the reduction of the roughness and amount of material removal. In the block where the samples are attached to there are internal channels. If this block is taken off, the aluminium sample underneath can be measured. It is expected that the polishing performance decreases with an increase in narrowness of the channels.

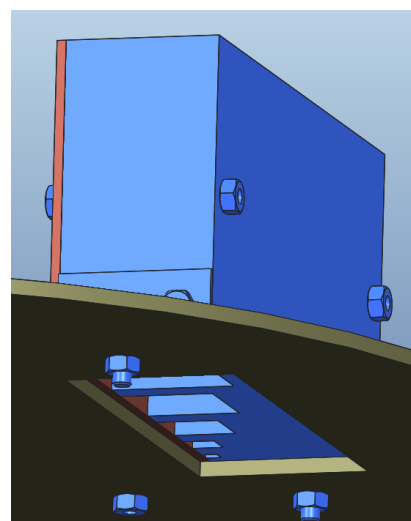
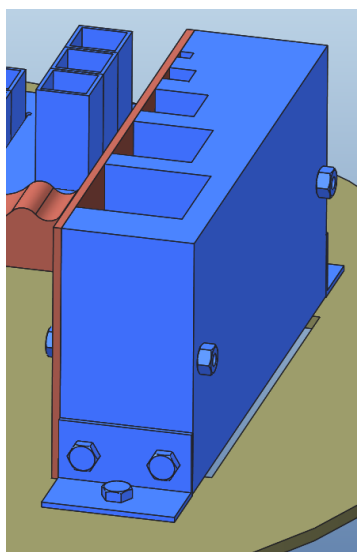


Figure 40- Set-up to test whether there is a difference in the result of polishing internal channels if the channel are orientated vertically

### *Verically orientated channels*

In Figure 40, a block is presented that is identical to the block in Figure 39, only this block is orientated vertically. The goal is to find potential differences in the results for polishing internal channels horizontally or vertically.

### **Initial measurements**

Previously to the polishing experiment the roughness and thickness of the samples is measured at the locations of interest. Some of the samples couldn't be measured with a micrometer since the spots of interest lay beyond the reach of this instrument. In this case, a height measuring instrument is used as depicted in Figure 41 left. In Figure 41 right a photograph is depicted of a roughness measurement in progress.



Figure 41: Left: measurement of thickness of sample with height measuring instrument. Right: measurement of roughness with the Perthometer C5D.

### **3.3.2 FUTURE TESTS**

Per polishing technique under research the planned future activities are laid out:

- Domeless rotary vibrator:

From the initial measurements it turned out that the roughness was out of spec. (not produced as requested). Therefore, the next step will be returning the samples and improve them in consultation with the manufacturers. As already stated, the samples that will be returned are made of aluminium and milled. The test will also be done with 3d printed materials to simulate both the ability of the process to polish milled and printed parts.

- Laser polishing and robotic supported polishing:

Up till now, we were not yet able to find partners to research both techniques. We will continue our effort to find suitable partners next year.

### 3.4 CAD -CAM

To post process the printed metal part with a CNC machine, the part needs to be properly positioned on the machine and the CNC code may need to be amended to get expected final shape. A 3D scanning approach has been proposed to detect the geometrical shape of the printed part as well as the location of the part on the machine. And then the result of scanning can be used for the amendment of CNC code for post-processing of the part via integrating with either CAM system or CNC system. Two different integration concepts have been proposed and their pros as well as cons have been compared in the report O1.1. According to the comparison of the proposed two concepts, the concept of integrating 3D scanning with CNC system presents more advantages due to the potential benefits it will deliver:

- The model comparison algorithm/method for NC code amendment can be integrated with the 3D scanning system to develop a universal tool for automatically positioning of the printed part onto an offline clamping system or the work table of a machine;
- The reference point is located/marked on the surface of the clamping system/work table where the surface can be the reference of work plane. This will make it be universal for any printed parts.
- With this concept, the CAM programming can be earlier or synchronized with the printing procedure which will significantly reduce the total time of the production.

A flow chart of the concept of integrating 3D scanning with CNC system is shown in Figure Figure 42.

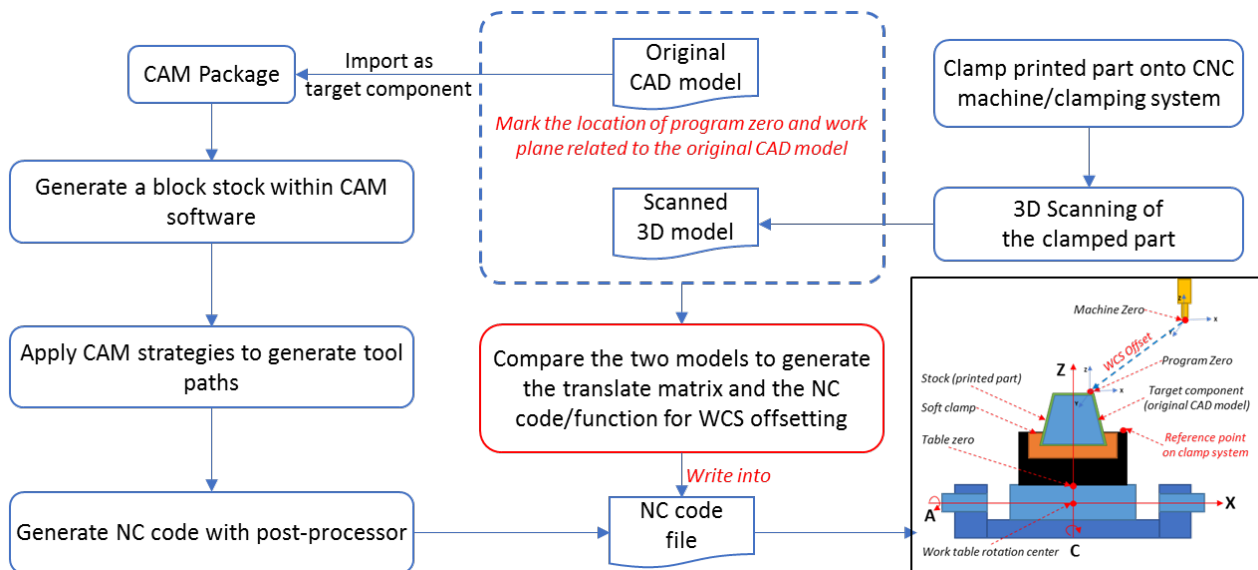


Figure 42: Concept of the integrating 3D scanning with CNC system

#### 3.4.1 Definition of the feasibility test

For the integration of 3D scanning and CNC system, one crucial step is to generate the translate matrix and the CNC code/function for WCS offsetting. Currently, there are various CNC machines with different CNC controllers. Considering the universality of our solution, a 5-axis (3+2) with rotary table configuration will be selected as the test machine and the standard G-Code is presumed be supported by CNC controller. The purpose of this feasibility test is to:

- Demonstrate the calculation of parameters used in G-Code functions for WCS offsetting based on results of comparison between the 3D scanned model and the original CAD model;

- Validate the calculation results through applying rotation on the rotary axis A and C of CNC machine.

To carry out the feasibility test, the configuration of CNC machine and a simple part is designed as shown in Figure 43. The post-processing of this part is to drill a hole with diameter of 10mm and deep of 10mm on the surface marked as green. The green surface is a rectangle where the hole is perpendicular to the surface and located at the centre of the rectangle surface.

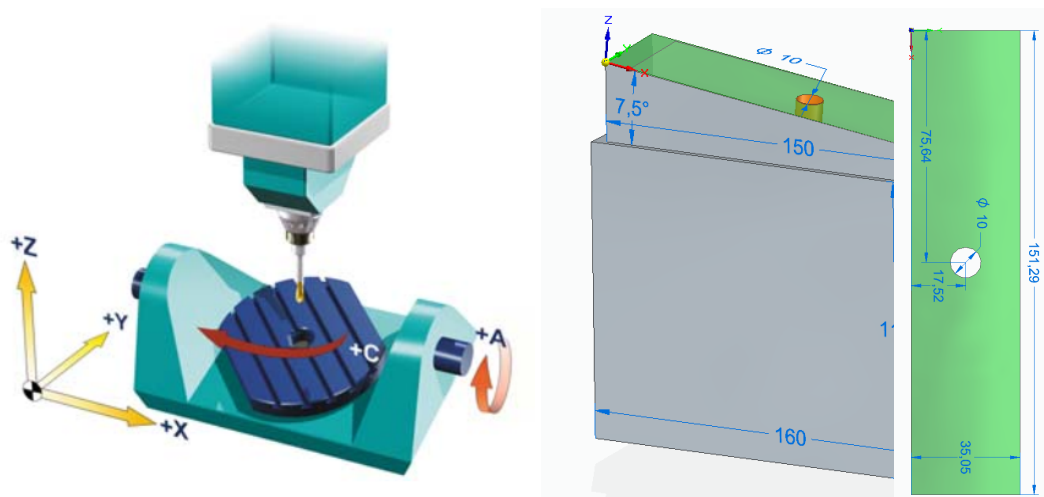


Figure 43: 3+2 CNC machine and dimension of the demo part

To drill this hole with a CNC machine, one of the simplest methods for CNC programming is to make the green surface as working plane and locate the workpiece coordinate system (WCS) zero at somewhere of the surface such as the corner of the rectangle as shown in Figure ?. The z-axis is perpendicular to the surface and x and y axis align with the edges of the rectangle. Within this WCS, the G Code to move the tool from zero point to the centre of the hole could be:

```
G0 X0Y0Z0 ; Move to program origin at 0, 0, 0
G91 ; Switch to relative coordinates
G0 X75.64Y17.52 ; Move to the centre of the hole
```

This G-Code should be work well only if the demo part was properly positioned on the machine to make the green surface be perpendicular to the Z-axis of CNC machine and the edge of the surface alignment with the X-axis of CNC machine at the same time. Further, the origin of the CNC machine has to be coincided with the origin of the workpiece. However, the green surface of the demo part is not parallel with its bottom surface which makes it difficult to guarantee that all the conditions can be satisfied during clamping for executing the above G-Code properly.

Fortunately, most modern CNC controllers provide functions for coordinate system transformation, working with titled working plane such as FANUC's G68.2, SIMENS' CYCLE800, and HEIDENHAIN's PLANE SPATIAL function. However, to use these advanced CNC functions, the value of critical parameters particular the rotation angles around relative axes have to be known through measurement or calculation.

### 3.4.2 Calculation of required parameters

For a 5-axis (3+2) CNC machine as shown in Figure 43, the rotation operations only can be applied to A-axis and C-axis. For a part clamped onto the rotatory table of CNC machine as illustrated in Figure 44, the first step is to make the working plane to be perpendicular to the Z-axis of the CNC machine through rotating around C- and A-axis. It is important to note that the centre of the rotation (MRZP) is the intersection point of C-axis and A-axis which is normally different with the intersection point of Z-axis and X-axis.

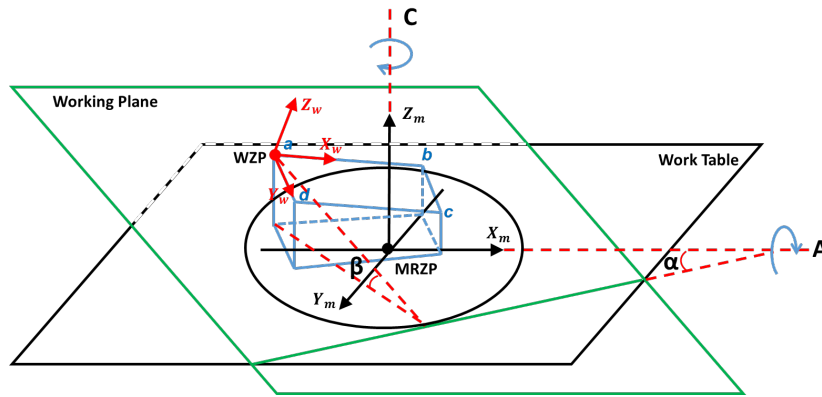


Figure 44: Illustration of a clamped part on a rotary table of CNC machine

Any working plane which is angled ( $\beta$ ) to the surface of worktable will intersect on a line with an angle ( $\alpha$ ) to the A-axis as illustrated as above. To make the working plane parallel to the surface of work table (machine's XY plane), the rotary table should rotate angle of  $\alpha$  around C-axis and title angle of  $\beta$  around A-axis. The value of  $\alpha$  and  $\beta$  can be calculated based on the normal of working plane within the machine's coordinate system. Given points  $a, b, c, d$  on the working plane, the normal of this working plane  $N$  can be calculated based on any three points. If the vector  $U = b - a$  and the vector  $V = d - a$  then the normal  $N = U \times V$  and can be calculated by:

$$\begin{bmatrix} N_x \\ N_y \\ N_z \end{bmatrix} = \begin{bmatrix} U_y V_z - U_z V_y \\ U_z V_x - U_x V_z \\ U_x V_y - U_y V_x \end{bmatrix} \quad (1)$$

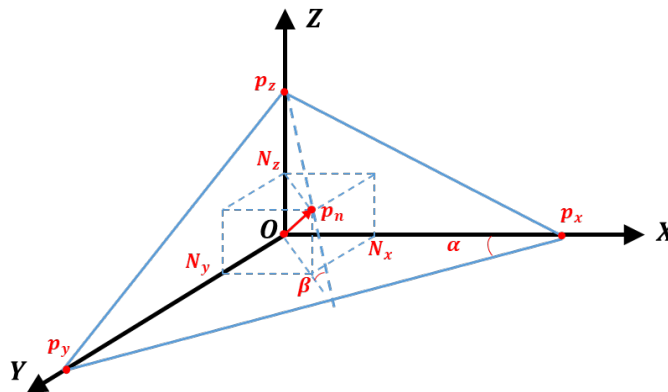


Figure 45: Illustration of a plane and its normal vector

The normal vector  $N$  is often normalized to unit length from the origin of the coordinate system  $O$  to the vector point  $p_n$  as shown in Figure 45. The plane contains the vector point intersects at point  $p_x, p_y, p_z$  respectively with axis X, Y, Z. Given the value of normal  $N = (N_x, N_y, N_z)$ , the value of angle  $\alpha, \beta$  can be calculated as following:

$$\alpha = \frac{\pi}{2} - \tan^{-1} \frac{N_y}{N_x} \quad (2)$$

$$\beta = \frac{\pi}{2} - \sin^{-1} N_z \quad (3)$$

The working plane should be perpendicular to the Z-axis of the CNC machine through rotating an angle of  $\alpha$  around C-axis and rotating an angle of  $\beta$  around A-axis respectively. However, the orientation of the X-axis and Y-axis used in CNC programming may different with the machine's X-axis and Y-axis. Additionally, the coordinate of the workpiece's programming origin will be changed due the rotation of C-axis and A-axis. Therefore, a further step is needed to calculate the real location of the programming origin in the machine's coordinate system for WCS offsetting and the angle between workpiece's X-axis/Y-axis and machine's X-axis/Y-axis for the rotation of WCS around machine's Z-axis.

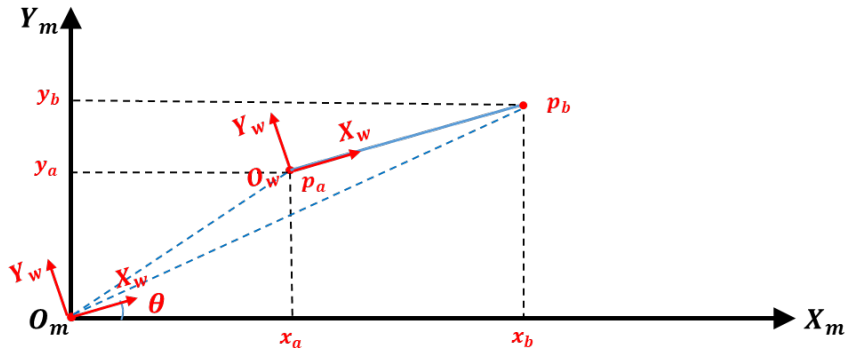


Figure 46: Illustration of the projection of working plane

After orthogonalizing of the working plane, the relationship between machine's XY plane and workpiece's XY plane can be illustrated as shown in Figure 46. Given a line from point  $p_a$  to  $p_b$  within the working plane, the location of these two points in the machine's XY plane can be represented as  $(x_a, y_a)$  and  $(x_b, y_b)$  respectively. While in the workpiece's XY plane, the line  $p_a p_b$  is parallel to the X-axis and the point  $p_a$  is the origin of XY plane. To align the workpiece's X-axis/Y-axis with the machine's X-axis/Y-axis, the working plane needs to be rotated with an angle of  $\theta$  around machine's Z-axis which can be calculated as following:

$$\theta = \tan^{-1} \frac{y_b - y_a}{x_b - x_a} \quad (4)$$

However, for a 5-axis (3+2) CNC machine configured with rotary table, there is no option to rotate the workpiece around machine's Z-axis if the A-axis not at its home position. Therefore, after orthogonalizing of the working plane, an alternative solution for alignment of X/Y-axis is to apply a rotation of coordinate system rather than rotate the workpiece physically. Additionally, the machine's origin should be matched with workpiece's origin through WCS offsetting before apply the rotation of coordinate system.

It is important to note that by now our operations are based on the coordinate system of rotary centre point (MRZP) rather than the home position of the machine (MZP). Given the initial location of workpiece's origin  $O_w(x_w, y_w, z_w)$  in the coordinate system of MRZP ( $WCS_{MRZP}$ ), after rotating angle of  $\alpha, \beta$  around C-axis and A-axis respectively, the new location of  $O'_w(x'_w, y'_w, z'_w)$  can be calculated as following:



$$\begin{bmatrix} x'_w \\ y'_w \\ z'_w \\ 1 \end{bmatrix} = \begin{bmatrix} \cos \alpha & -\sin \alpha & 0 & 0 \\ \sin \alpha & \cos \alpha & 0 & 0 \\ 0 & 0 & 1 & 0 \\ 0 & 0 & 0 & 1 \end{bmatrix} \cdot \begin{bmatrix} 1 & 0 & 0 & 0 \\ 0 & \cos \beta & -\sin \beta & 0 \\ 0 & \sin \beta & \cos \beta & 0 \\ 0 & 0 & 0 & 1 \end{bmatrix} \cdot \begin{bmatrix} x_w \\ y_w \\ z_w \\ 1 \end{bmatrix} \quad (5)$$

Providing that the location of MRZP in the machine's coordinate system ( $WCS_{MRZP}$ ) is  $(x_r, y_r, z_r)$ , then the offset of  $X, Y, Z$  between machine's origin and workpiece's origin can be calculated as following:

$$\begin{bmatrix} O_X \\ O_Y \\ O_Z \end{bmatrix} = \begin{bmatrix} x_r \\ y_r \\ z_r \end{bmatrix} + \begin{bmatrix} x'_w \\ y'_w \\ z'_w \end{bmatrix} \quad (6)$$

### 3.4.3 Validation of the proposed method

To validate the method proposed above, a demo part as shown in Figure 3.4.2 was studied through a simulation based approach. The surface marked in green colour of the demo part needs to be processed and be defined as the working plane. As shown in Figure 47, the demo part was clamped onto the rotary table and the working plane is angled to the machine's XY plane. The initial position of the C-axis and A-axis is illustrated where the C-axis parallel to the machine's Z-axis and A-axis parallel to the machine's X-axis.

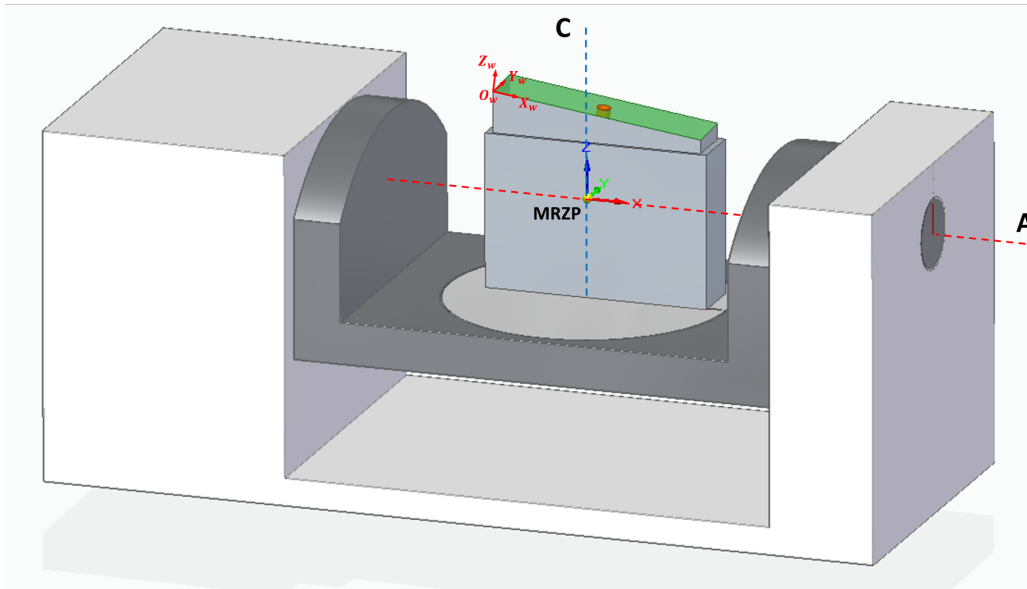


Figure 47: Illustration of the initial position of rotary table with clamped demo part

Figure 3.4.6. Illustration of the initial position of rotary table with clamped demo part

The location of workpiece's origin can be obtained through 3D scanning the clamped demo part at the initial position and then comparing with the original CAD model used for CNC programming. For the scanned 3D model, the coordinate system should be located at the intersection point of C-axis and A-axis, and the X, Y, Z axis should be align with machine's A-axis, Y-axis, C-axis respectively. After that, the working plane and the origin for CNC programming can be defined on the scanned 3D model based on the comparison (model registration) result.

For this demonstration, the location of workpiece's origin  $O_w$  in  $WCS_{MRZP}$  was measured with value of  $(-68.31, 0.55, 69.48)$  and the normal of the working plane was measured with value of  $(0.13, -0.05, 0.99)$ . According to formulation (2) and (3), the rotation angle  $\alpha, \beta$  around C-axis and A-axis respectively can be calculated as following:

$$\alpha = \frac{\pi}{2} - \tan^{-1} \frac{-0.05}{0.13} = 1.94 \quad (110.04^\circ)$$

$$\beta = \frac{\pi}{2} - \sin^{-1} 0.99 = 0.14 \quad (8.11^\circ)$$

Based on the calculation results, the rotation around C-axis and A-axis was applied on the simulation model as shown in Figure 48 where the working plane is exactly perpendicular to the machine's Z-axis.

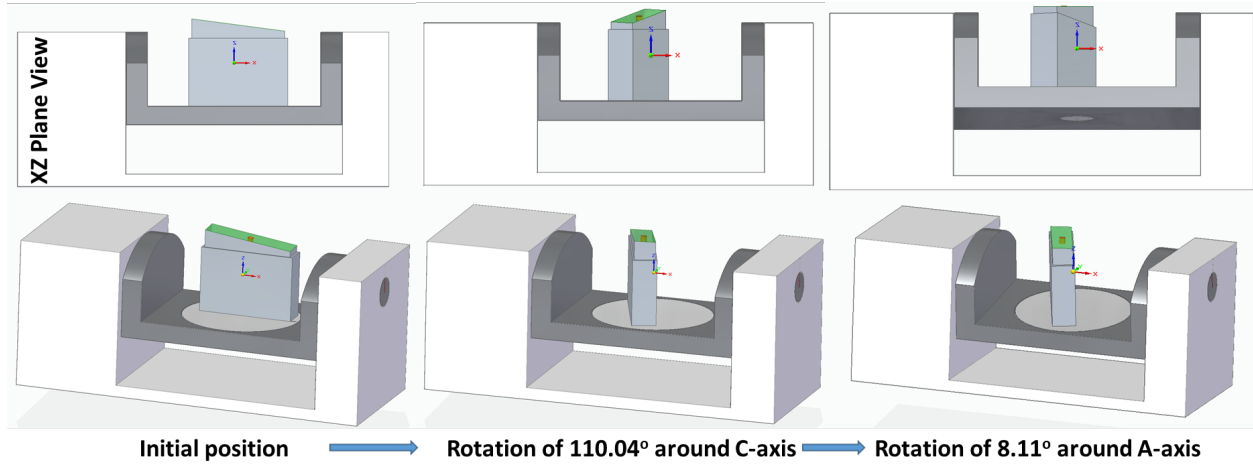


Figure 48: Results of rotation of  $\alpha$ ,  $\beta$  around C-axis and A-axis

From the top view, the orientation of workpiece's X-axis is angled of  $70.18^\circ$  with machine's X-axis as shown in Figure 49. Therefore, to align the workpiece's X and Y axis with machine's X and Y axis, the coordinate system needs to be rotated anticlockwise around machine's Z-axis at angle of  $180 - 70.18 = 109.82^\circ$ . Further, the location of workpiece's origin ( $O_w$ ) after rotation was measured with value of ( $x_w = 22.89$ ,  $y_w = -73.52$ ,  $z_w = 59.70$ ) which can be used for offsetting of the machine's origin position.

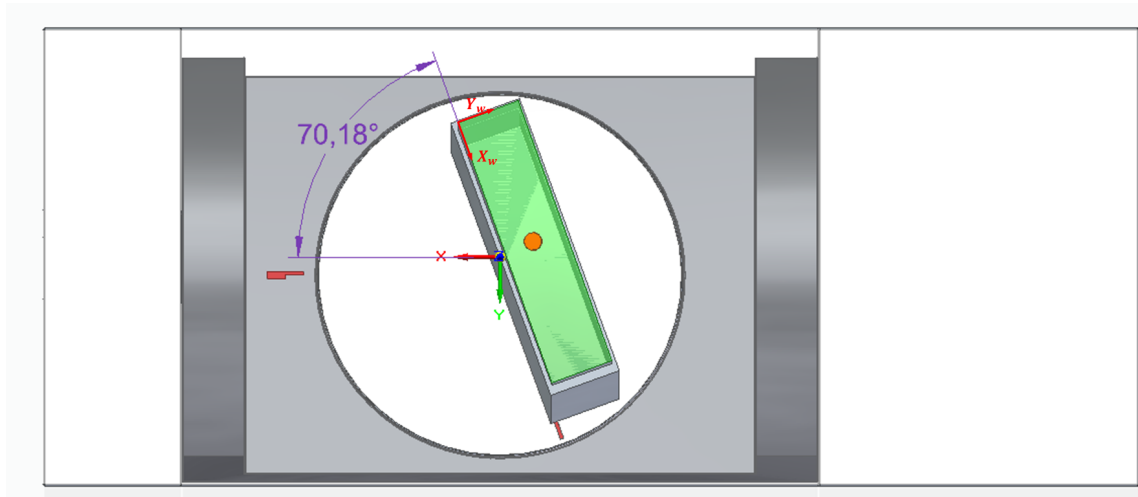


Figure 49: Top view of the clamped demo part after rotation



## 4 CONCLUSION

This document describes the feasibility tests, performed to determine the feasibility and risks of different concepts of the post processing steps (clamping, scanning, polishing and CAD/CAM) to reduce cost and time. For the selection the Technology Readiness Level (TRL) was an important selection criterion. Only technologies were selected that have a TRL level of at least 5.

### Fast prototyping approach:

Initial “Fast Prototyping Approach” results show, it is feasible to create new offset values based on scanned data. However, this approach is CNC machinery depended and therefore not generic.

Assessment of the current CNC machinery and software available today will be done to find a more flexible solution, in line with the 3D&FPP project objectives.

Assumed eligible strategies to update CNC machinery offset values, which will be further investigated, are e.g:

- Update the coordinate system in the CAM program
- Update the specific G-code parameters in the post processed machine code

These strategies will be compared in a trade off table.

### Clamping

Feasibility tests were performed with 3 different clamping solutions. This gave the following results:

- A special interface that is printed on the product

Initial experiments showed that it is possible to print clamping interfaces to printed objects. This gives more freedom in orientation to clamp the object compared to re-using support + baseplate orientation for clamping.

- Hot melts

Hot melt are found that are most likely strong enough to hold the object in place while milling. The young's modulus of the material is however quite low and does not allow applying a thick layer around the printed object and obtain sufficient stiffness.

- Softclamp based on bed of fins

A Matrix clamp was obtained to perform more tests. Initial experiments seem promising of the technology. A part of the product is however covered with the clamping tool and cannot be milled.

The TRL level of the hot melt route is qualified as relatively low. This didn't qualify this technology as main path for this project.

The preferred solution to proceed with, is the special interface printed on the product and/or in combination with the softclamp based on a bed of fins.

### Scanning

A combination of GOM ScanBox 5120 and ATOS TripleScan III 16 MP with 560 mm measuring volume was used for scanning a 3D printed use case of the project. Measurements showed that the technology seems to meet the requirements for the project.

### Polishing

As far as polishing is concerned, based on the current research and theory, robotic supported polishing and domeless rotary vibration as a means for post process surface treatment (with desired and reproducible surface roughness and geometry tolerance levels) are the most eligible techniques. Both techniques will be part of the next steps within the 3D&FPP project.

### CAD/CAM

The crucial algorithm to calculate the parameters required by integration of 3D scanning techniques with CNC system for the flexible post-processing of 3D printed metal parts was developed and validated through a simulation-based approach. The feasibility test results indicated, that the algorithm is able to generate the location of workpiece's origin and the normal of working plane within the scanned 3D model. This information can be used for rotating of the rotary table (via A-axis and C-axis) to make the working plane be perpendicular to the machine's Z-axis (tool axis). Further, the new location of the workpiece's origin within machine's coordinate system can be calculated which will be used for offsetting of the machine's origin. With the validated integration method, potential benefits can be delivered including:

- CNC programming can be implemented before obtain the printed part which will save significant time;
- The algorithm to calculate parameters required for CNC machine is based on the limited capability of 5-axis CNC machine, so that any 3-axis milling machine with an additional rotary table will be able to perform the job;
- The developed algorithm can be integrated with available 3D scanning software such as GOM or be developed as an independent software tool to connect the 3D scanning system and CNC system.

Further investigation will be carried out in the future for the integration of the developed algorithm with 3D model comparison algorithm. Also, a software prototype will be considered to apply the developed algorithms with a friendly graphical user interface.

## 5 ANNEXES

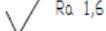
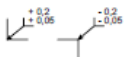
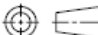
### 5.1 LIST OF FIGURES

Figure 1 left; the Fast Prototype object during fabrication by using a 5 axis CNC milling machine at Hitech Bihca. Right: The object during 3D scanning by using a robotized measuring cell at Argon measuring solutions .....	9
Figure 2: Concept with printing a extra handle to the product. ....	11
Figure 3: concept of handle to usercase products. Left: the Hinge, Right the mirror object. ....	11
Figure 4: Model of mirror object with handle .....	12
Figure 5: deformations due to 1 N force. The deformation is $0.38\mu\text{m}$ . ....	12
Figure 6: first eigenfrequency mode is 889Hz. ....	13
Figure 7: printed products on base plate. Before removing support structures .....	13
Figure 8: Left: mirror object without handle; middle:, Mirror object with handle and struts interface; right: mirror object with solid handle. ....	13
Figure 9: Elcometer Adhesion Tester. ....	15
Figure 10: model of mirror object on a layer of hot melt .....	17
Figure 11: Deformations due to a force of 10 N .....	18
Figure 12: required adhesion forces for 10N force. Left the tension forces( $0.06\text{MPa}$ ) Right: shear force $0.01\text{MPa}$ ) .....	18
Figure 13: Model of mirror object in a bucket of material .....	19
Figure 14: Deformations. Remind the deformations are scaled. The max movement is red and is $0.5\mu\text{m}$ . Sliding rough surfaces. ....	19
Figure 15: With high adhesion between the bottom of the mirror object, the deformation is 67 nm. ....	20
Figure 16: concept of clamping with a thermoplast .....	20
Figure 17: Result clamping simulation using a thermoplast clamp .....	21
Figure 18: Anton Paar MCR301 Rheometer. ....	21
Figure 19: Bed of pins clamp by <a href="http://www.matrix-innovations.com">www.matrix-innovations.com</a> .....	23
Figure 20: Matrix-innovation clamp with (polymer) user case of the mirrorblock. ....	24
Figure 21: clamping a product with only 1 clamp. After fixing the pins, the shape of the product is visible and the product can be placed back again .....	24
Figure 22 clamping rectangular under an angle .....	25
Figure 23: Matrix innovation clamp bought by TNO .....	25
Figure 24: variation on baseplate concept / printing on standard clampplate .....	26
Figure 25: product plate is fixed by screws to the base plate. ....	27
Figure 26: with printing of the product, also reference planes are printed for easy alignment with postprocessing .....	27
Figure 27: user case: mirror object. ....	28
Figure 28: measurement repeatability between 10 measurements .....	29
Figure 29: schematic explanation of the matrix computation. ....	30
Figure 30: test setup .....	30
Figure 31: orientation compensation and transformation matrix calculation .....	31
Figure 32: initial state – top plane of is not horizontal .....	32
Figure 33: After compensation – top plane is horizontal. ....	32
Figure 34 - In this figure the threaded rod and bolt are denoted which are used to clamp the product to the stationary bed of the machine. ....	34
Figure 35 -Overview of the complete test assembly. ....	34

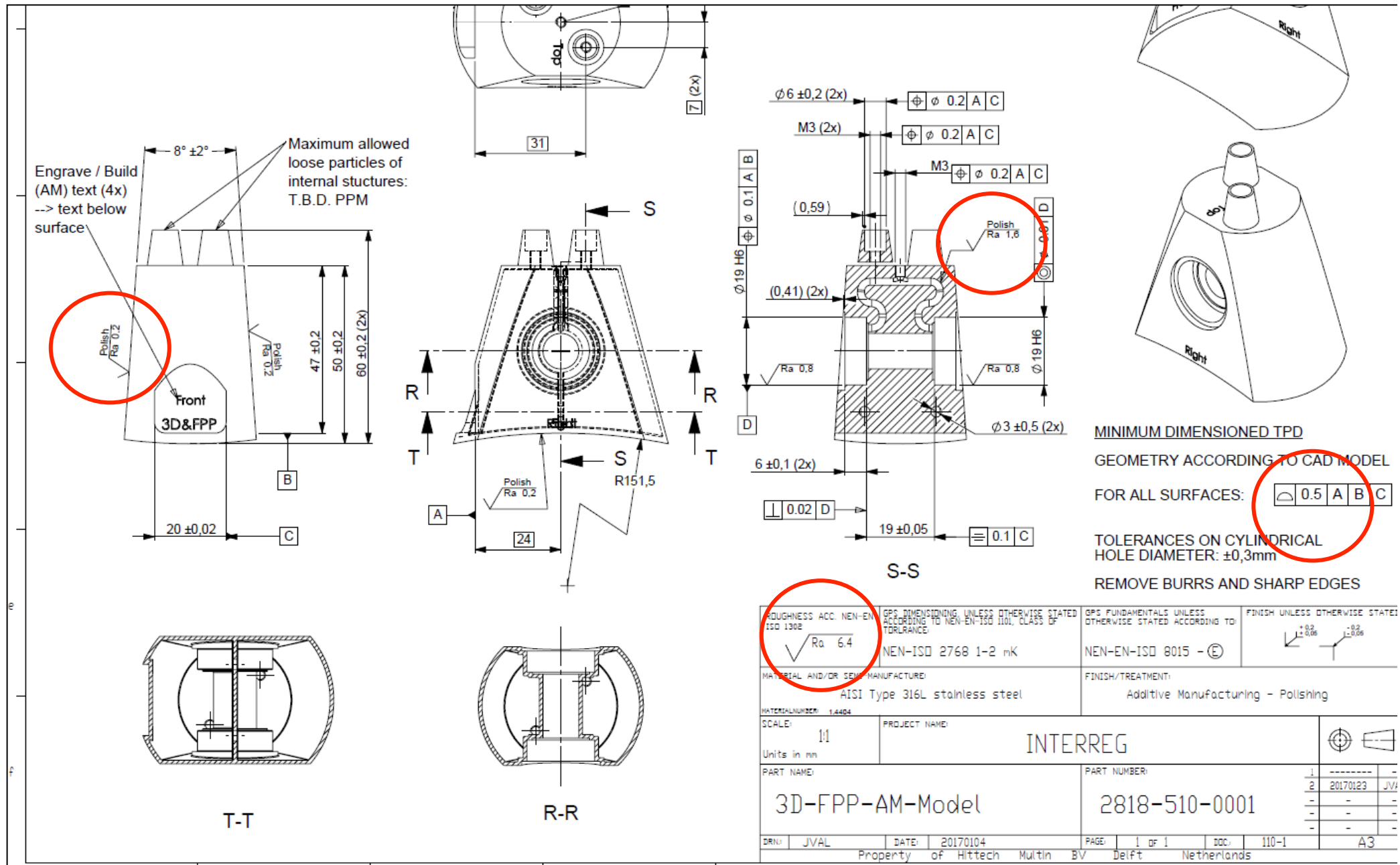
Figure 36 –assy to test the performance when polishing cavities. The red plate is the actual sample that is measured. The blue weld-assy simulates the cavities in a product.....	35
Figure 37 - Test sample to compare the polishing result for products with differently curved surfaces .....	35
Figure 38- Resulting roughness is measured as a function of x.....	36
Figure 39 - Set-up to investigate difference when polishing different materials and analyse how well internal channels can be polished. ....	37
Figure 40- Set-up to test whether there is a difference in the result of polishing internal channels if the channel are orientated vertically.....	37
Figure 41: Left: measurement of thickness of sample with height measuring instrument. Right: measurement of roughness with the Perthometer C5D. ....	38
Figure 42: Concept of the integrating 3D scanning with CNC system .....	39
Figure 43: 3+2 CNC machine and dimension of the demo part.....	40
Figure 44: Illustration of a clamped part on a rotary table of CNC machine .....	41
Figure 45: Illustration of a plane and its normal vector.....	41
Figure 46: Illustration of the projection of working plane.....	42
Figure 47: Illustration of the initial position of rotary table with clamped demo part.....	43
Figure 48: Results of rotation of $\alpha$ , $\beta$ around C-axis and A-axis.....	44
Figure 49: Top view of the clamped demo part after rotation .....	44

## 5.2 LIST OF TABLES

Table 1: trade off table with clamping concepts. ....	10
Table 2 Advantages and disadvantages extra handles. ....	14
Table 3: adhesion tests. The candidate materials( except for the 3798 LM) are tested, and also some other materials. ....	16
Table 4: mechanical material property.....	22
Table 5: Advantages and disadvantages of hotmelts .....	22
Table 6 Advantages and disadvantages Bed of pins. ....	26
Table 7 Advantages and disadvantages extra baseplate. ....	27

ROUGHNESS ACC. NEN-EN ISO 1302 		GPS DIMENSIONING UNLESS OTHERWISE STATED ACCORDING TO NEN-EN ISO 1101, CLASS OF TOLERANCE: NEN-ISO 2768 1-2 mK		GPS FUNDAMENTALS UNLESS OTHERWISE STATED ACCORDING TO: NEN-EN-ISO 8015 - (E)		FINISH UNLESS OTHERWISE STATED: 										
MATERIAL AND/OR SEMI-MANUFACTURE: Mould steel 1.1730				FINISH/TREATMENT: See note												
MATERIAL NUMBER: 1.1730																
SCALE: 1:2 Units in mm		PROJECT NAME: Interreg 3D&FPP														
PART NAME: Hscase-Corkscrew				PART NUMBER: 2818-510-0003												
				<table><tr><td>1</td><td>-----</td><td>-</td></tr><tr><td>-</td><td>-</td><td>-</td></tr><tr><td>-</td><td>-</td><td>-</td></tr></table>				1	-----	-	-	-	-	-	-	-
1	-----	-														
-	-	-														
-	-	-														

## 6.2 APPENDIX A.2: DRAWING GEARBOX DESIGN



## Fokker Hinge demonstrator

### General Tolerances:

- Overall dimensions:  $\pm 0,5$  mm
- Wall and flange thickness:  $\pm 0,2$  mm
- Surface roughness:  $Ra=3,2$   $\mu m$

### Specific tolerances:

Assembly faces:

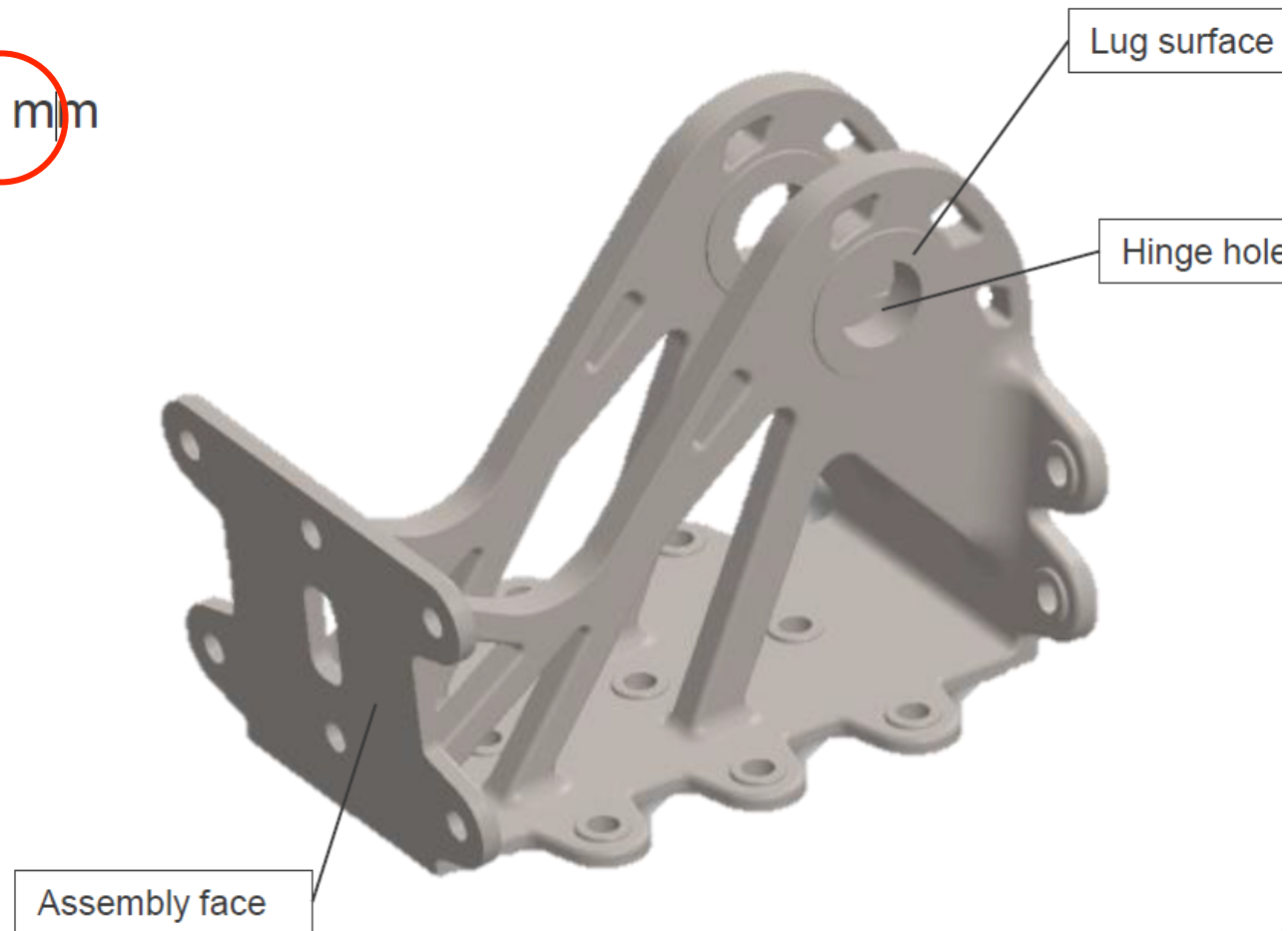
Position surface profile  $\Delta 1$  mm

Hinge hole:

Hole diameter: H7

Concentricity  $\odot \varnothing 0,1$  mm $\oplus$

Perpendicularity  $\perp \varnothing 0,1$  mm



[illegible]



